QUANTUM MONTE CARLO FOR NEUTRINO-NUCLEUS SCATTERING

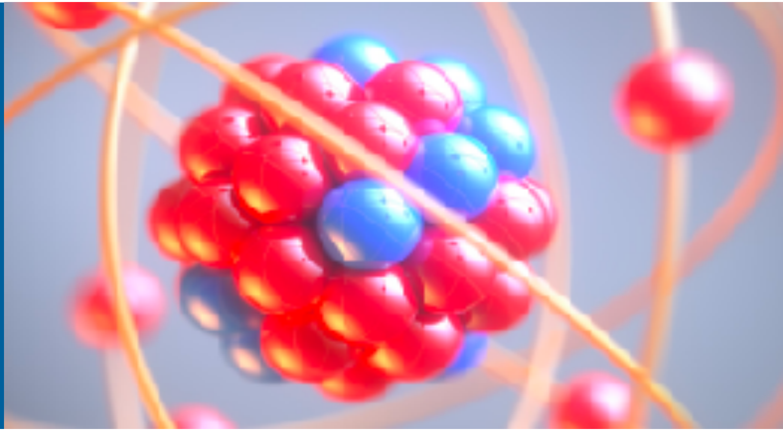

ALESSANDRO LOVATO

TIFPA Trento Institute for Fundamental Physics and Applications

Argonne NATIONAL LABORATORY

Neutrino Scattering at Low and Intermediate Energies

Mainz, June 29, 2023

COLLABORATORS

Argonne National Laboratory — C. Adams, B. Fore, K. Raghavan

Washington University in St. Louis — L. Andreoli, S. Pastore, M. Piarulli,

EPFL — G. Carleo, J Nys, G. Pescia

Los Alamos National Laboratory — J. Carlson, S. Gandolfi

Michigan State University — J. Kim, M. Hjorth-Jensen

Fermilab — N. Rocco, M. Wagman, N. Steinberg

INTRODUCTION

Accurate neutrino-nucleus scattering calculations critical for the success of the experimental program

$$N_{\rm near} \approx \int dE\, \Phi_{\rm near}(E) \times \underline{\sigma(E)}$$

$$N_{\rm far} \approx \int dE\, P(E) \times \Phi_{\rm far}(E) \times \underline{\sigma(E)}$$

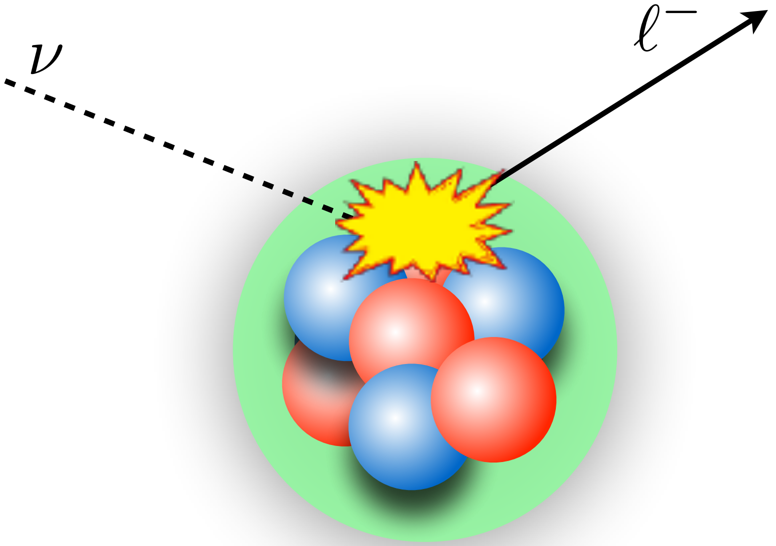

INTRODUCTION

If observed, $0\nu\beta\beta$ would show that lepton number is not conserved and that the neutrino mass has a Majorana component;

- Provide crucial information about neutrino mass generation;
- Suggest that the matter-antimatter asymmetry in the universe originated in leptogenesis;

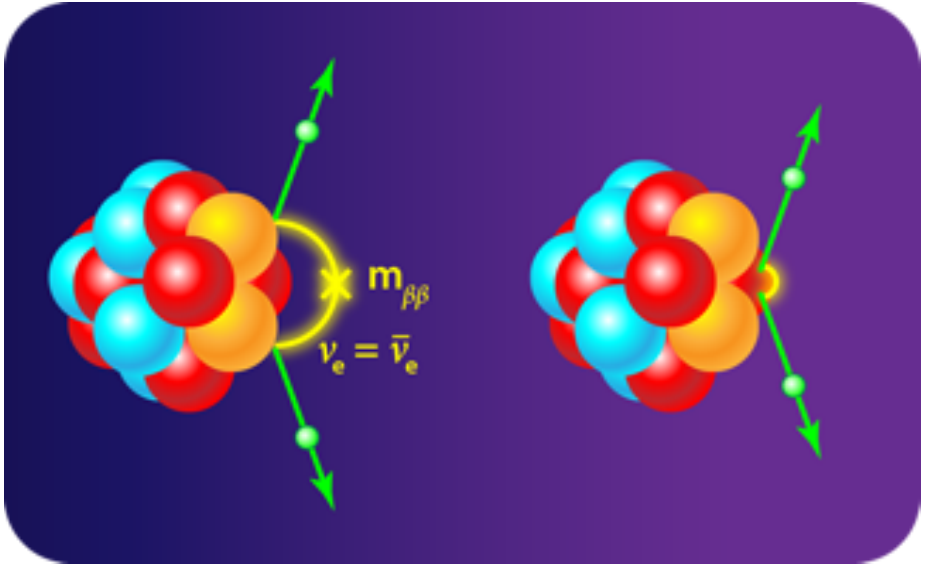

INTRODUCTION

The nuclear matrix elements is needed to extract the effective light-neutrino Majorana mass

$$[T_{1/2}]^{-1} = G^{0\nu}|M^{0\nu}|^2\langle m_{\beta\beta}\rangle^2 \quad ; \quad m_{\beta\beta} = \left|\sum_k m_k U_{ek}\right|^2 \quad ; \quad M^{0\nu} = \langle\Psi_f|O^{0\nu}|\Psi_i\rangle$$

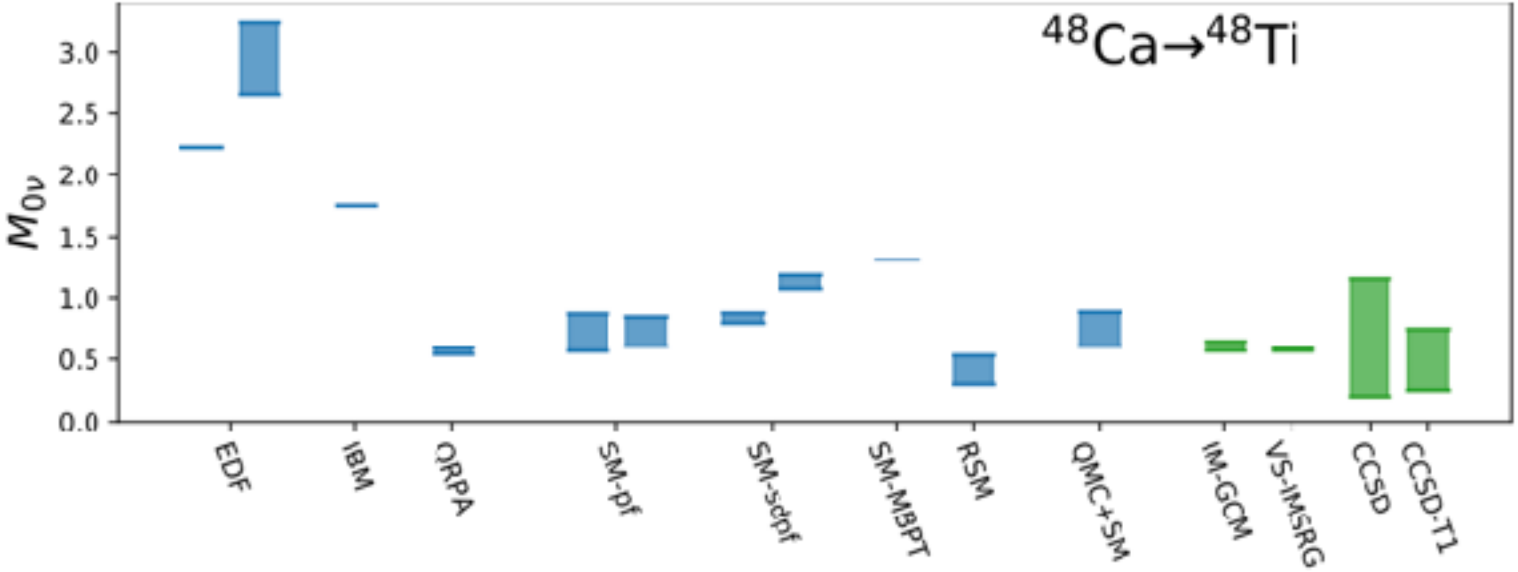

INTRODUCTION

An accurate understanding of nuclear dynamics is critical for multi-messenger astronomy

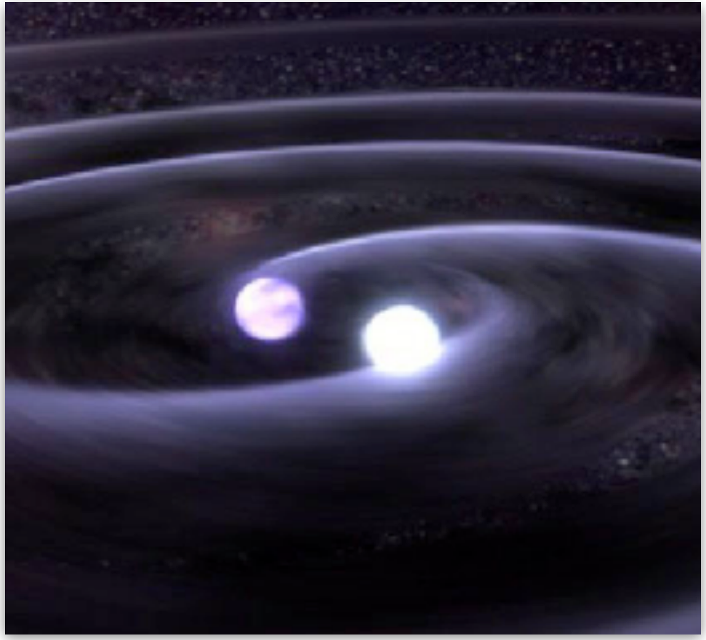

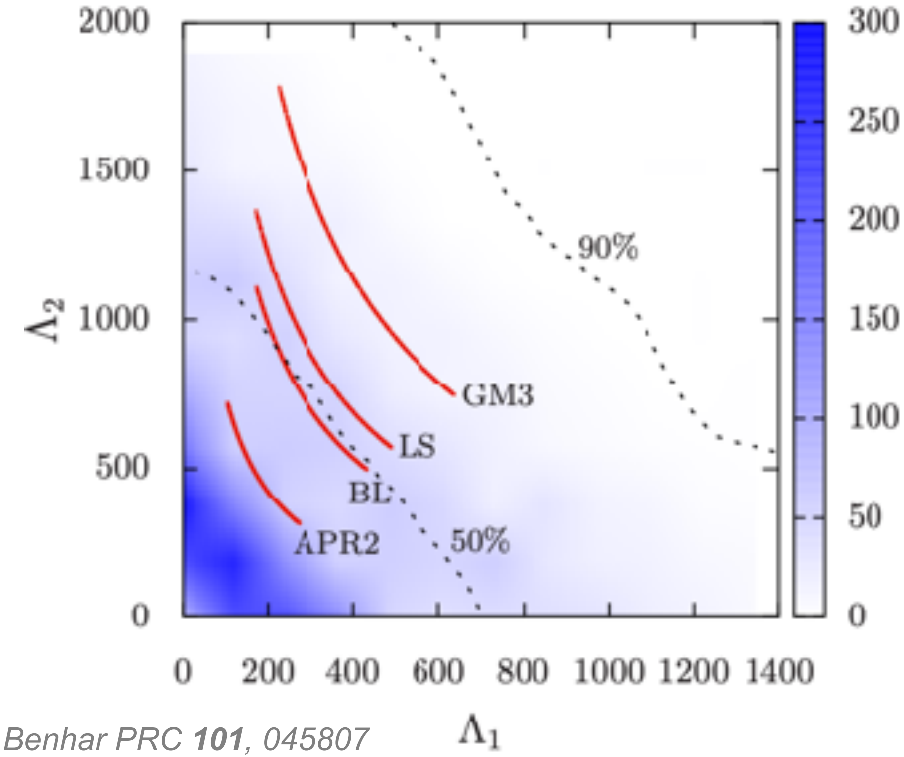

A. Sabatucci, O. Benhar PRC **101**, 045807

THE NUCLEAR MANY-BODY PROBLEM

In the low-energy regime, quark and gluons are confined within hadrons and the relevant degrees of freedoms are protons, neutrons, and pions

Effective field theories are the link between QCD and nuclear observables.

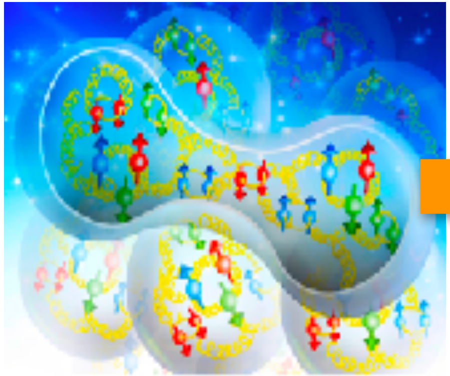

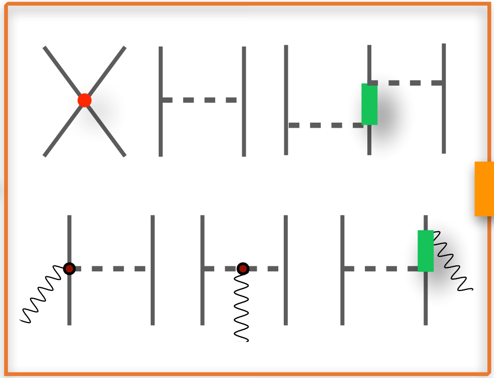

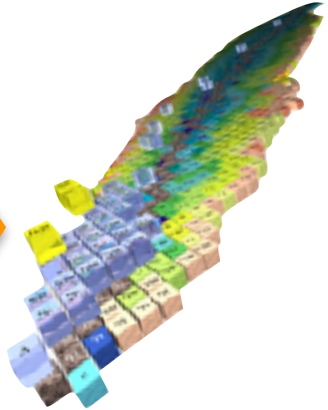

$$H = \sum_i \frac{\mathbf{p}_i^2}{2m} + \sum_{i<j} v_{ij} + \sum_{i<j<k} V_{ijk}$$

$$J = \sum_i j_i + \sum_{i<j} j_{ij}$$

THE NUCLEAR MANY-BODY PROBLEM

Chiral EFT exploits the broken chiral symmetry of QCD to construct potentials and consistent currents

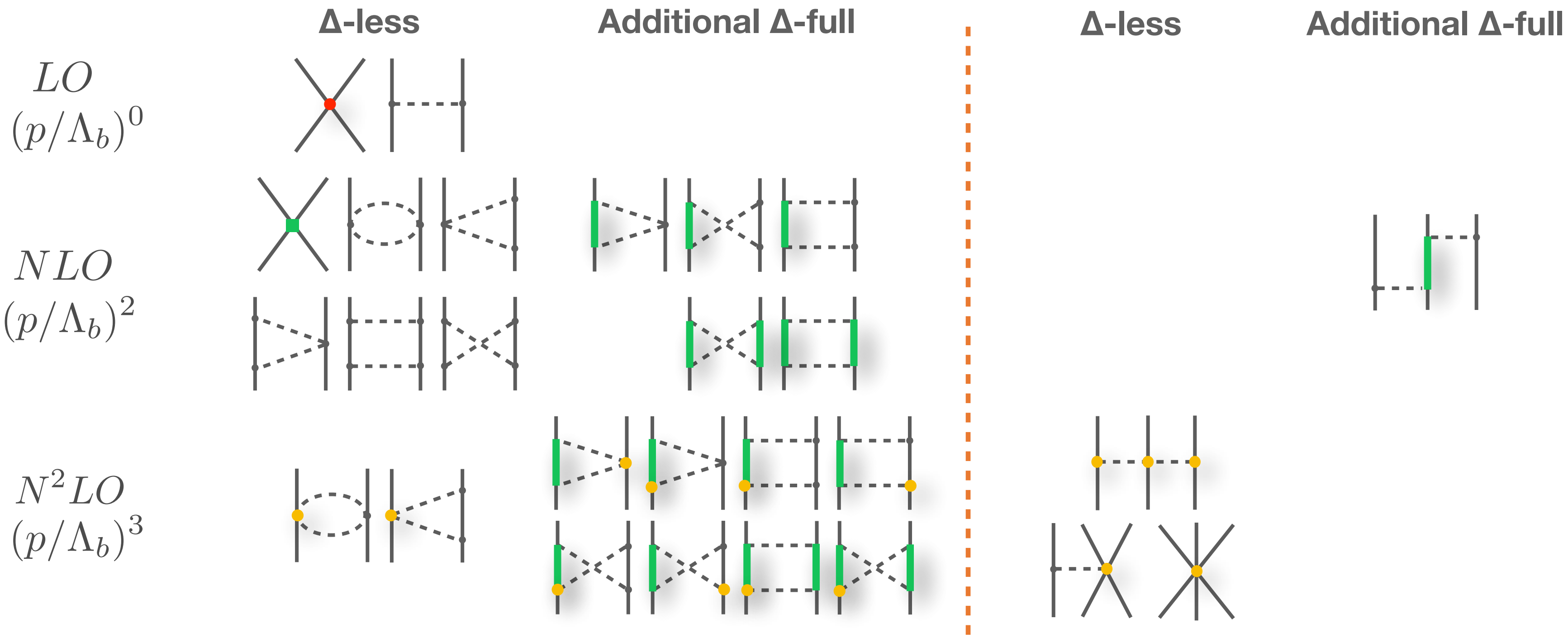

R. Machleidt et al., Phys. Scripta ***91****, 083007 (2016)*

M. Piarulli et al., Front.in Phys. ***7****, 245 (2020)*

THE NUCLEAR MANY-BODY PROBLEM

Non relativistic many body theory aims at solving the many-body Schrödinger equation

$$H\Psi_0(x_1,\dots,x_A) = E_0\Psi_0(x_1,\dots,\dots,x_A) \quad \longleftrightarrow \quad x_i \equiv \{\mathbf{r}_i, s_i^z, t_i^z\}$$

- Nuclear potentials are non-perturbative and spin-isospin dependent

$$H = \sum_i \frac{\mathbf{p}_i^2}{2m} + \sum_{i<j} v_{ij} + \sum_{i<j<k} V_{ijk} \quad \left\{ \begin{aligned} & v_{ij} = \sum_{p=1}^{18} v^p(r_{ij}) O_{ij}^p \\ & O_{ij}^{p=1,8} = (1, \sigma_{ij}, S_{ij}, \mathbf{L}\cdot\mathbf{S}) \times (1, \tau_{ij}) \end{aligned} \right.$$

- Nucleons are fermions, so the wave function must be anti-symmetric

$$\Psi_0(x_1,\dots,x_i,\dots,x_j,\dots,x_A) = -\Psi_0(x_1,\dots,x_j,\dots,x_i,\dots,x_A)$$

QUANTUM MONTE CARLO

The Green's function Monte Carlo uses imaginary-time projection techniques to extract the ground-state of the system from the trial wave function

$$\lim_{\tau\to\infty} e^{-(H-E_0)\tau}|\Psi_T\rangle = \lim_{\tau\to\infty}\sum_n c_n e^{-(E_n-E_0)\tau}|\Psi_n\rangle = c_0|\Psi_0\rangle$$

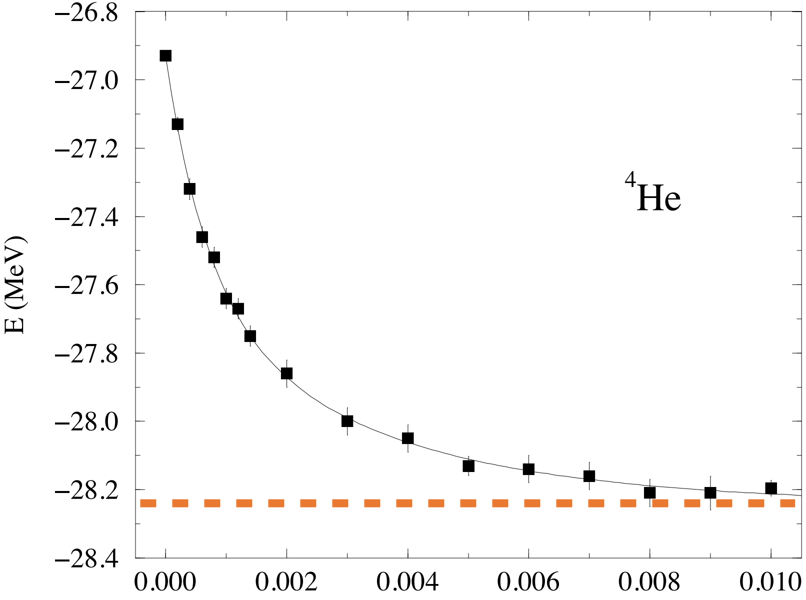

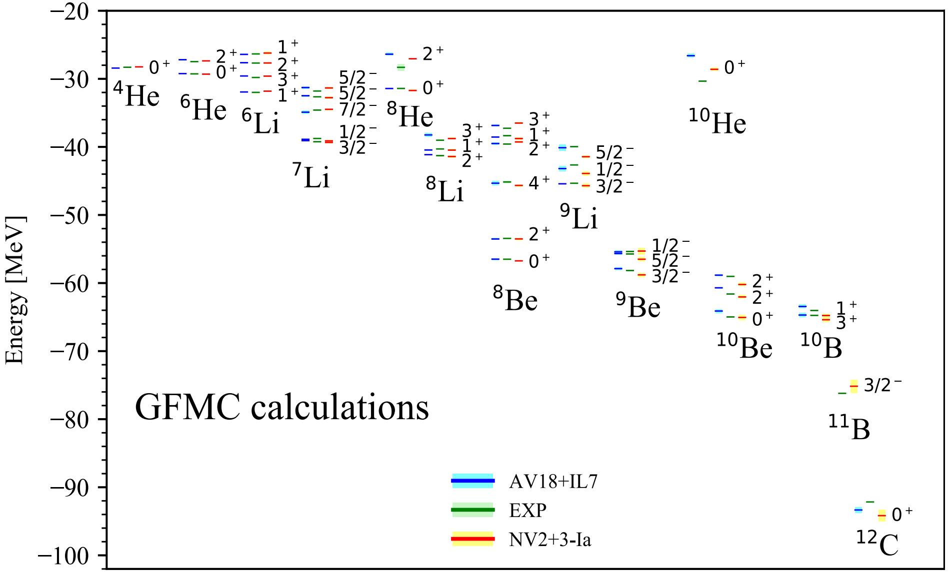

NEUTRINO-NUCLEUS SCATTERING

The inclusive cross section is characterized by a variety of reaction mechanisms

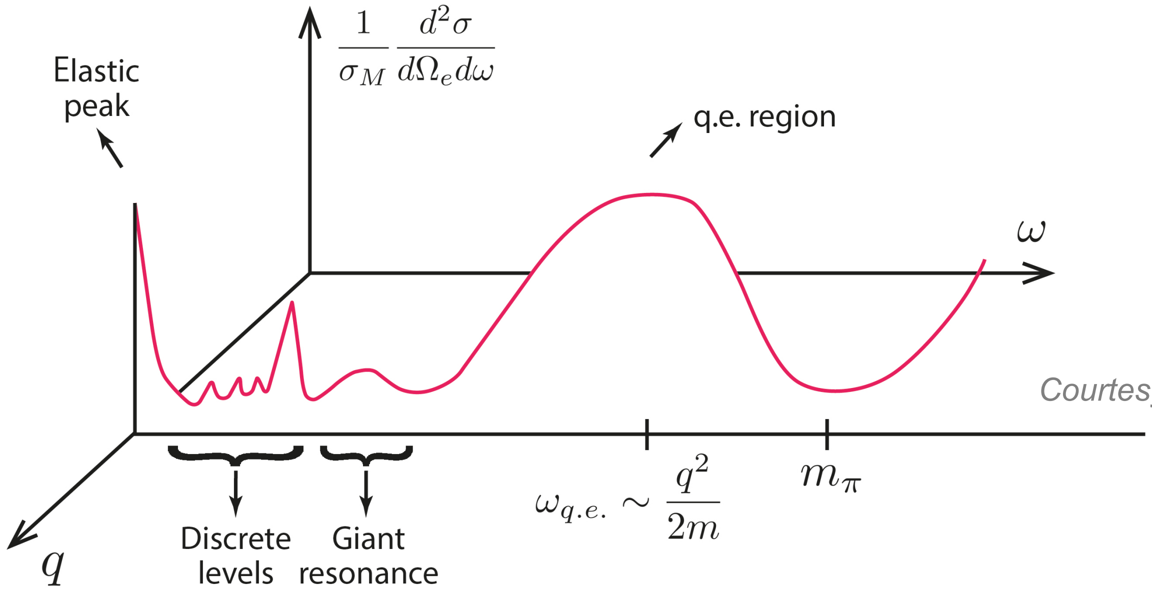

Courtesy of S. Pastore

The response functions contain all nuclear-dynamics information

$$R_{\alpha\beta}(\omega, \mathbf{q}) = \sum_f \langle\Psi_0|J_\alpha^\dagger(\mathbf{q})|\Psi_f\rangle\langle\Psi_f|J_\beta(\mathbf{q})|\Psi_0\rangle\delta(\omega - E_f + E_0)$$

EUCLIDEAN RESPONSES

Our GFMC calculations rely on the Laplace kernel

$$E_{\alpha\beta}(\tau,\mathbf{q}) \equiv \int d\omega e^{-\omega\tau} R_{\alpha\beta}(\omega,\mathbf{q})$$

At finite imaginary time the contributions from large energy transfer are quickly suppressed

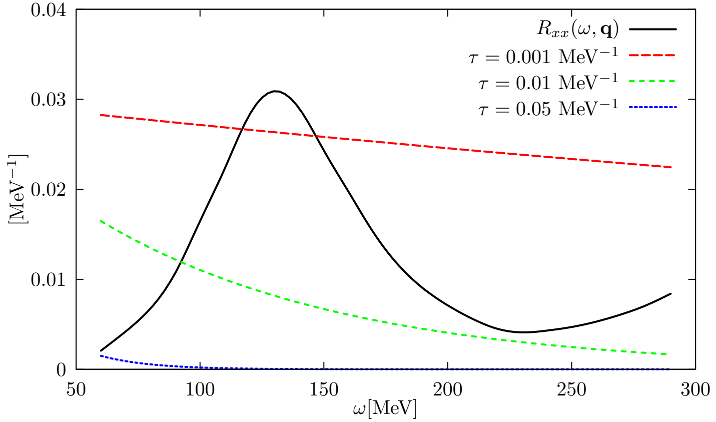

The system is first heated up by the transition operator. Its cooling determines the Euclidean response of the system

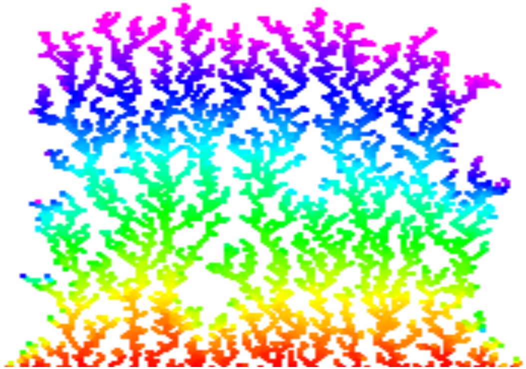

$$E_{\alpha\beta}(\tau,\mathbf{q}) = \langle\Psi_0|J_\alpha^\dagger(\mathbf{q})e^{-(H-E_0)\tau}J_\beta(\mathbf{q})|\Psi_0\rangle$$

$$\sum_f |\Psi_f\rangle\langle\Psi_f|$$

EUCLIDEAN RESPONSES

The integral transform of the response function is defined as

$$E_{\alpha\beta}(\sigma,\mathbf{q}) \equiv \int d\omega K(\sigma,\omega) R_{\alpha\beta}(\omega,\mathbf{q})$$

$$= \sum_f \int d\omega K(\sigma,\omega) \langle \Psi_0 | J_\alpha^\dagger(\mathbf{q}) | \Psi_f \rangle \langle \Psi_f | J_\beta(\mathbf{q}) | \Psi_0 \rangle \delta(\omega - E_f + E_0)$$

Using the completeness of the final states, it is expressed as a ground-state expectation value

$$E_{\alpha\beta}(\sigma,\mathbf{q}) = \langle \Psi_0 | J_\alpha^\dagger(\mathbf{q}) K(\sigma, H - E_0) J_\beta(\mathbf{q}) | \Psi_0 \rangle$$

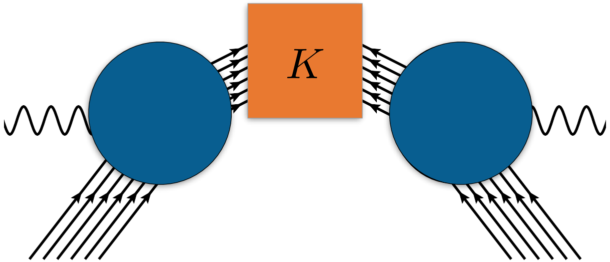

BEYOND ^{12}C: AFDMC AND MACHINE LEARNING

Inverting the Euclidean response is an ill posed problem: any set of observations is limited and noisy and the situation is even worse since the kernel is a smoothing operator.

$$E_{\alpha\beta}(\tau, \mathbf{q}) \longrightarrow R_{\alpha\beta}(\omega, \mathbf{q})$$

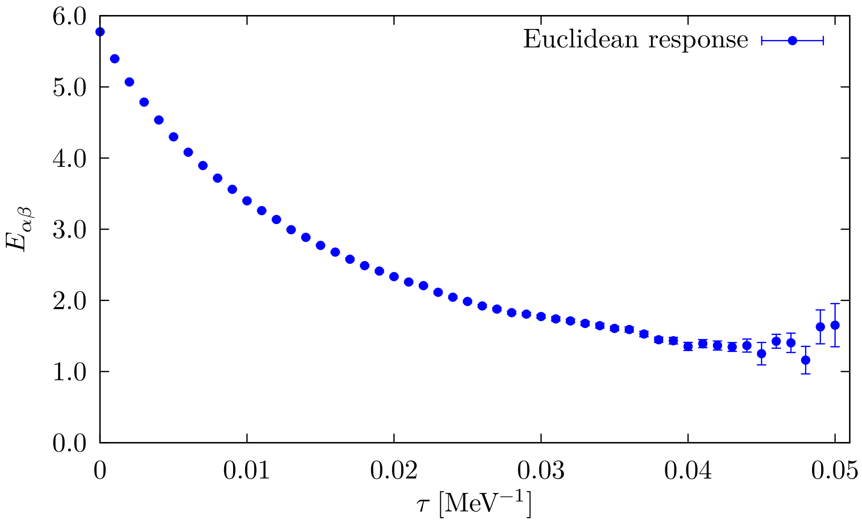

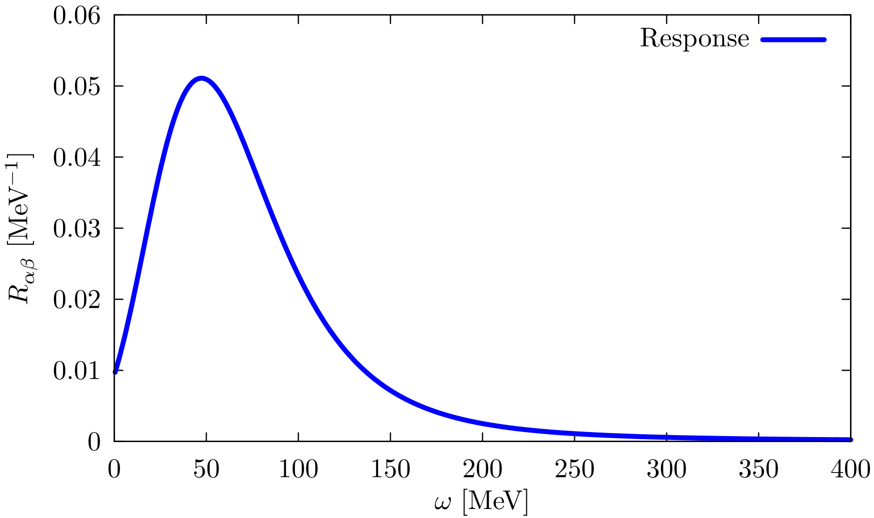

We find Maximum-entropy techniques to be reliable enough for quasi-elastic responses

VALIDATION WITH ELECTRON SCATTERING

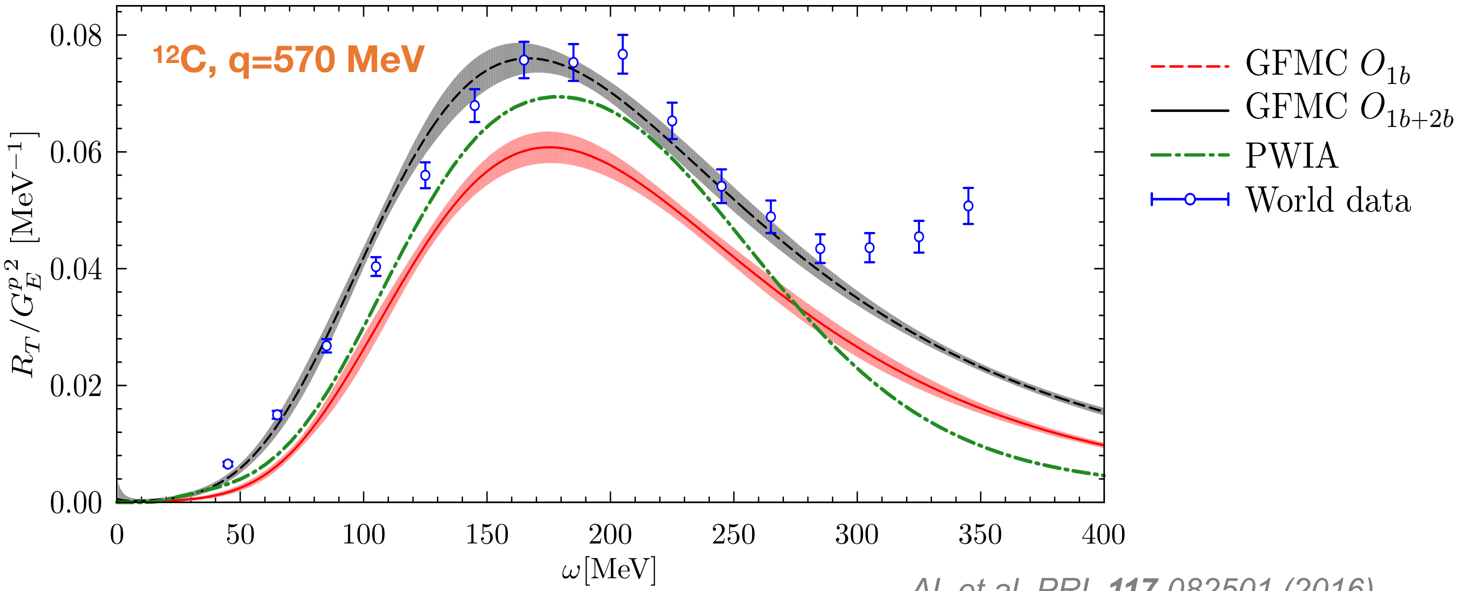

*AL et al. PRL **117** 082501 (2016)*

Two-body currents generate additional strength in over the whole quasi-elastic region

Correlations redistribute strength from the quasi-elastic peak to high-energy transfer regions

MINIBOONE CROSS SECTIONS

*AL et al., PRX **10**, 031068 (2020)*

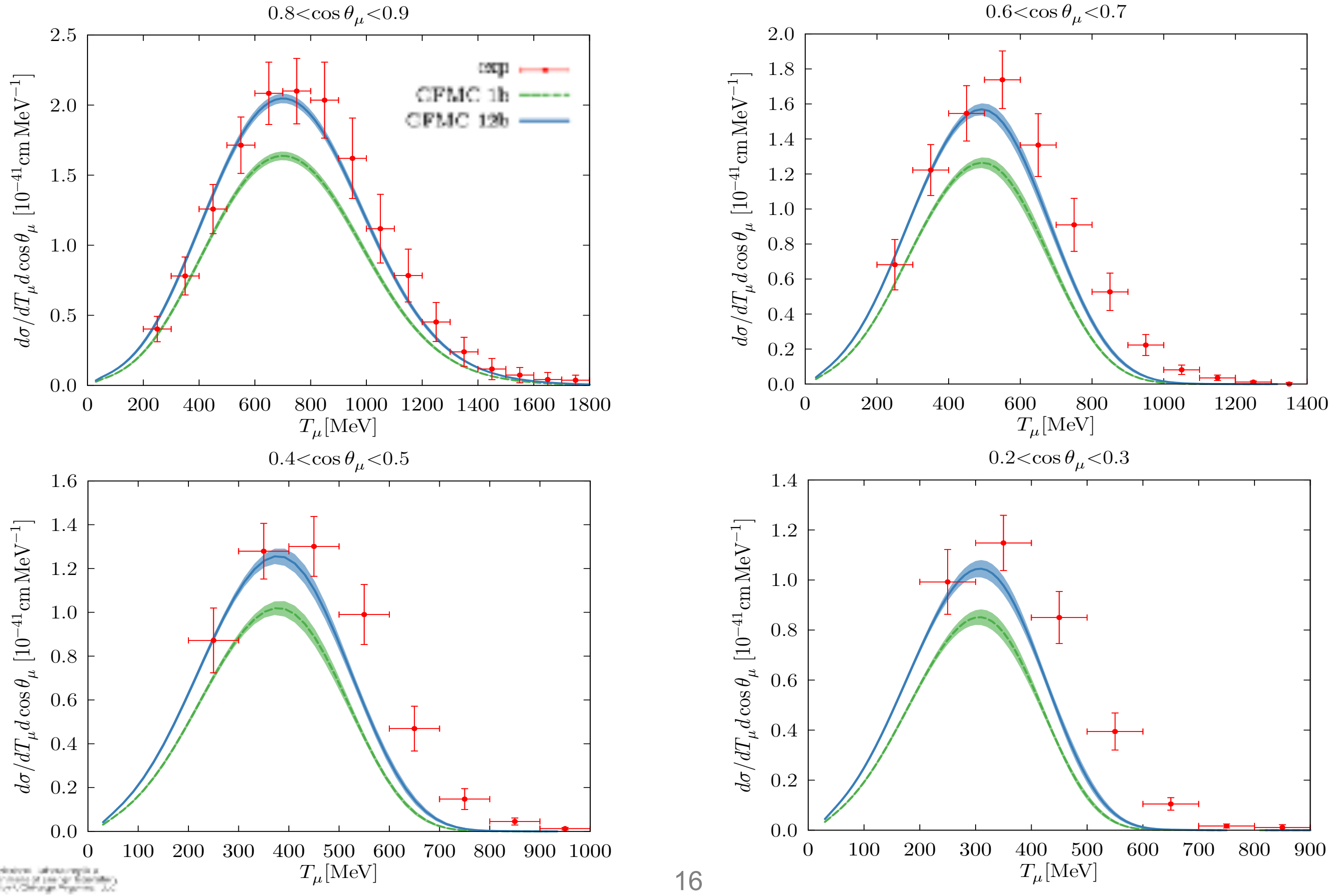

T2K CROSS SECTIONS

*AL et al., PRX **10**, 031068 (2020)*

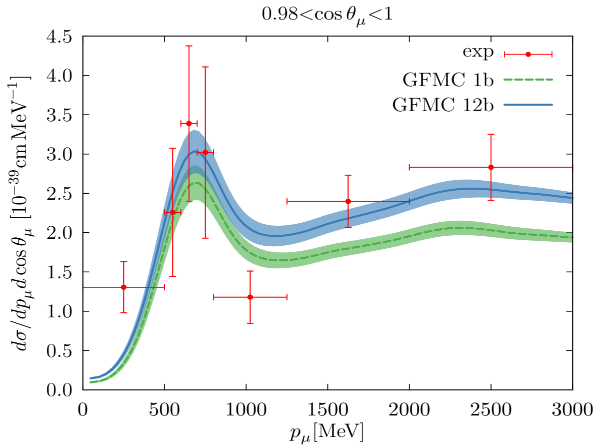

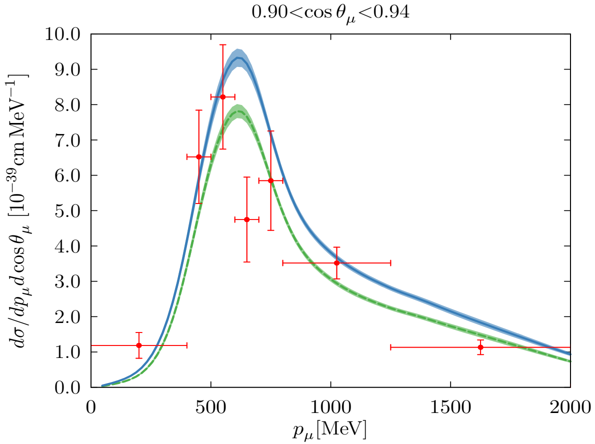

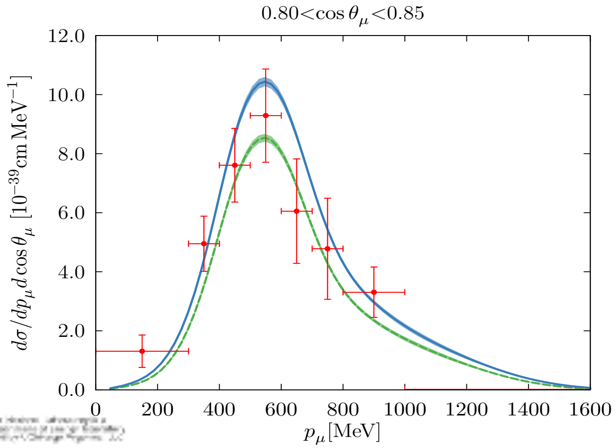

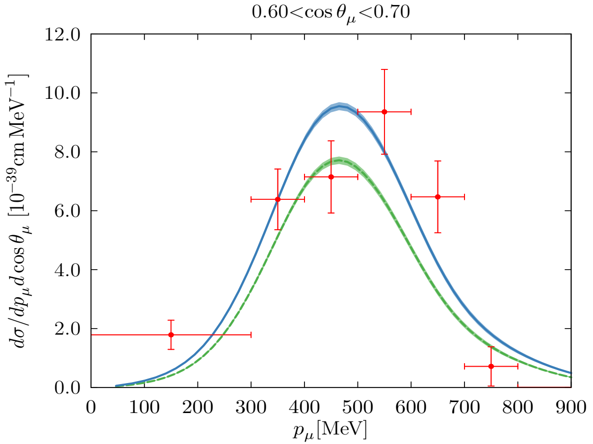

AXIAL FORM FACTOR

A precise knowledge of the **nucleon's axial-current form factors** is crucial for modeling neutrino-nucleus interactions;

Scarce (old) experimental data available

↕

Lattice-QCD calculations are essential

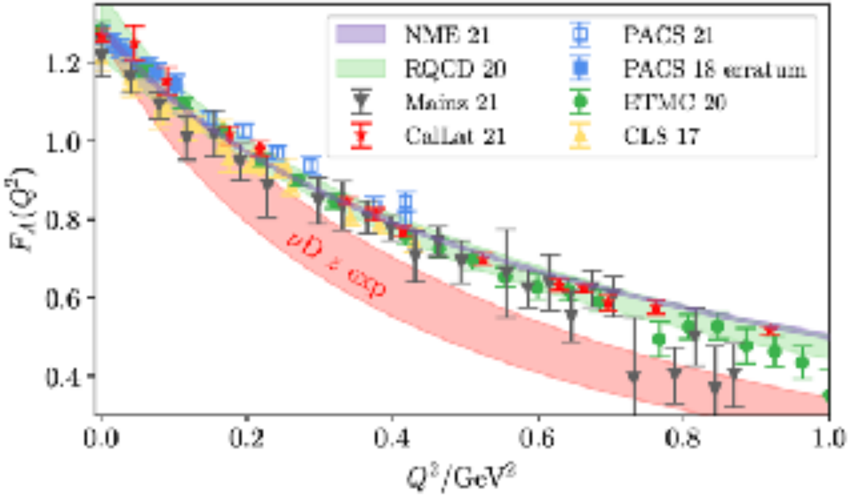

A. Meyer et al., arXiv:2201.01839

We have considered a value of the axial mass more in line with recent LQCD determinations

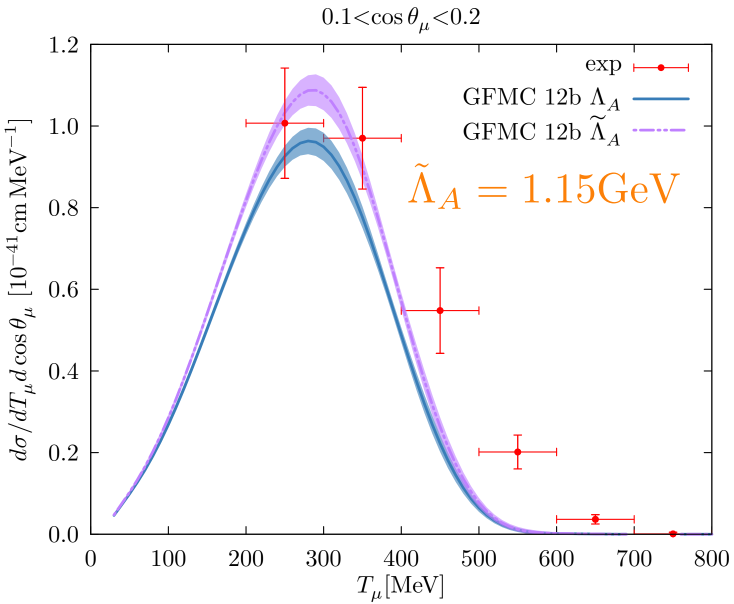

*AL et al., PRX **10**, 031068 (2020)*

AXIAL FORM FACTOR, CAREFUL ANALYSIS

We employed z-expansion parameterizations of axial form factors, consistent with experimental or LQCD data

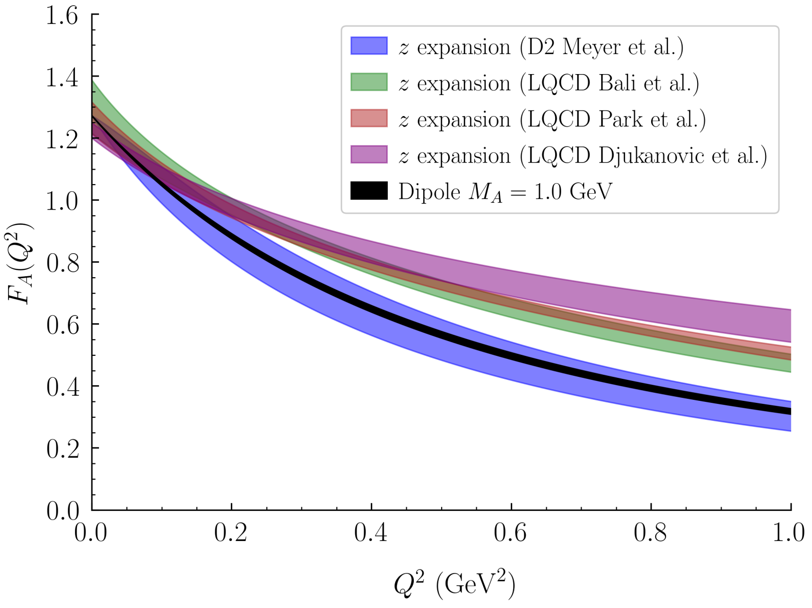

D. Simons, et al, arXiv:2210.02455

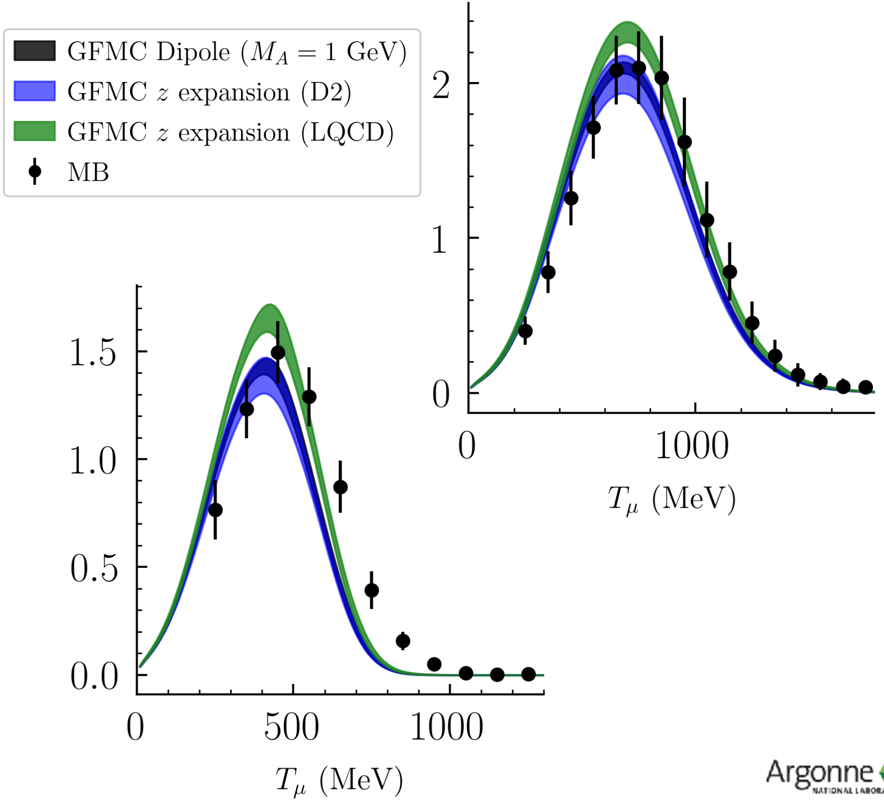

EXPONENTIAL SCALING

Green's function Monte Carlo uses all spin-isospin components of the wave function

$$|S\rangle = \begin{pmatrix} s_{\uparrow\uparrow\uparrow} \\ s_{\uparrow\uparrow\downarrow} \\ s_{\uparrow\downarrow\uparrow} \\ s_{\uparrow\downarrow\downarrow} \\ s_{\downarrow\uparrow\uparrow} \\ s_{\downarrow\uparrow\downarrow} \\ s_{\downarrow\downarrow\uparrow} \\ s_{\downarrow\downarrow\downarrow} \end{pmatrix}$$

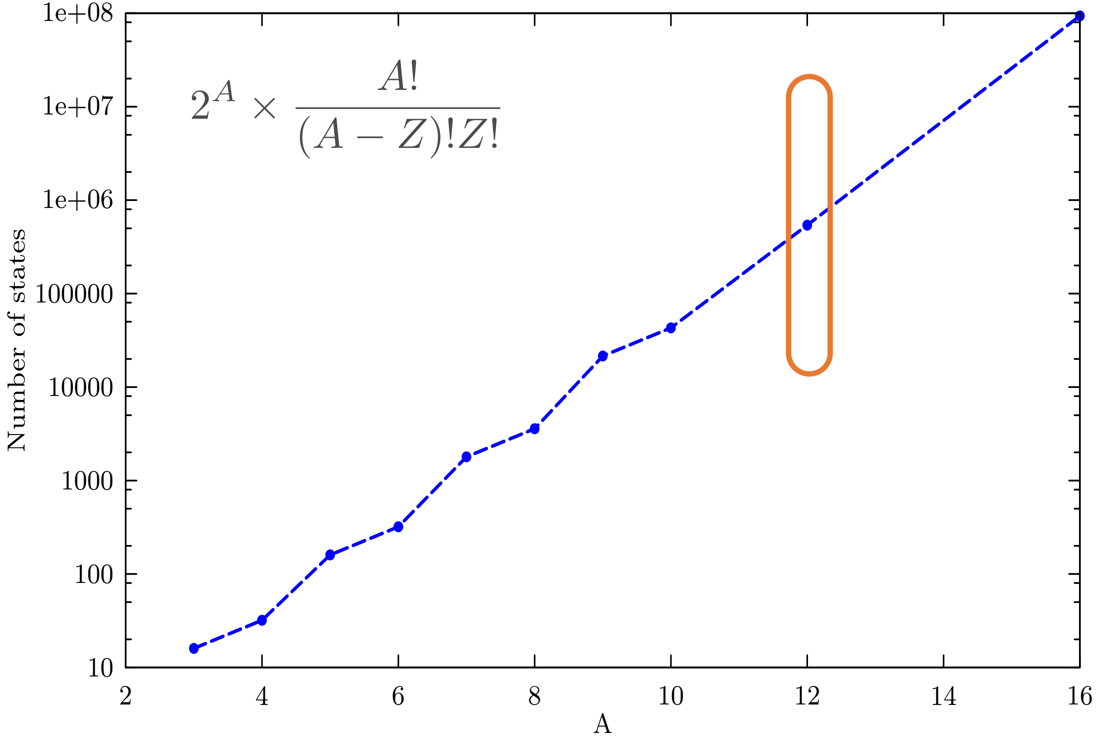

HOW TO TACKLE LARGER NUCLEI?

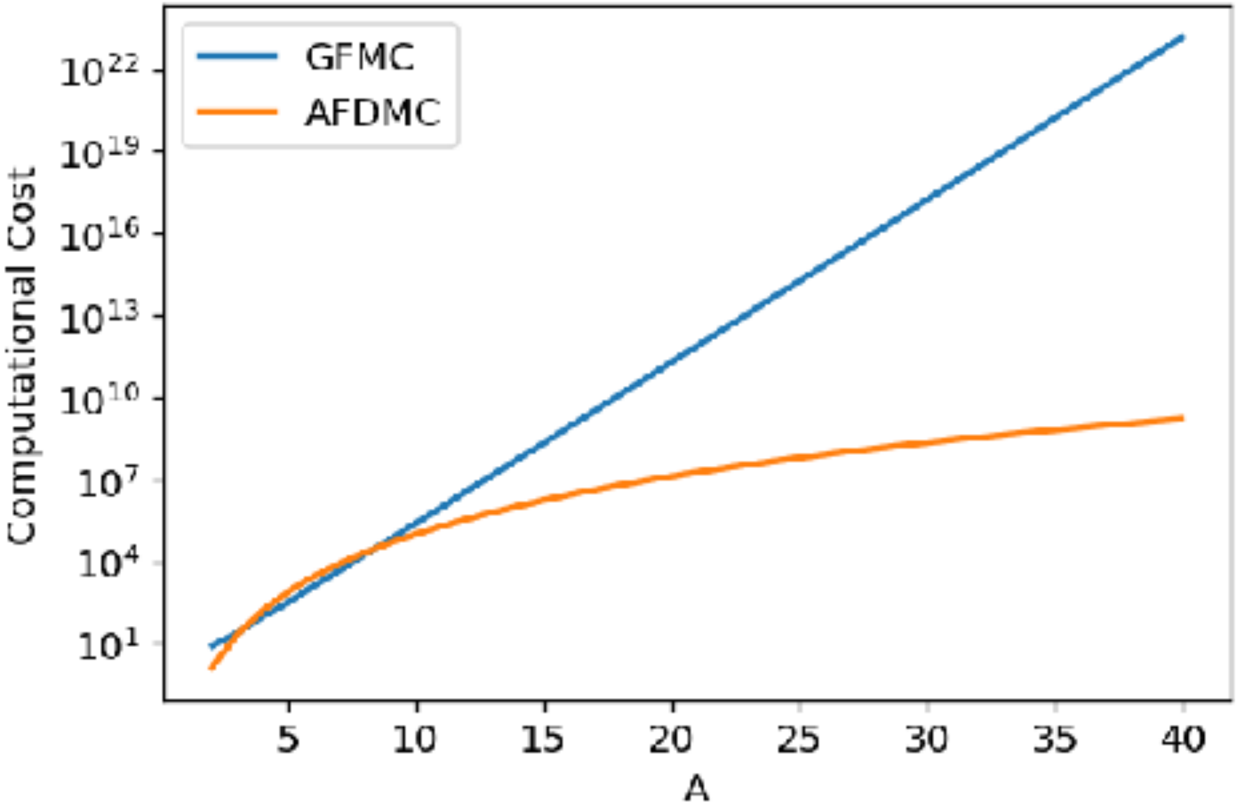

BEYOND ^{12}C: AFDMC AND MACHINE LEARNING

The auxiliary-field diffusion Monte Carlo method can treat ^{16}O sampling the spin-isospin

We developed the AFDMC to allow for the calculation of Euclidean response functions

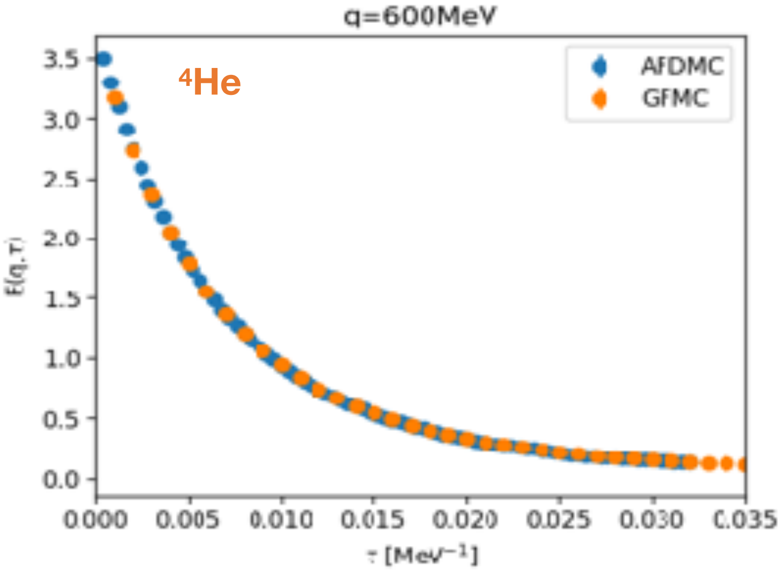

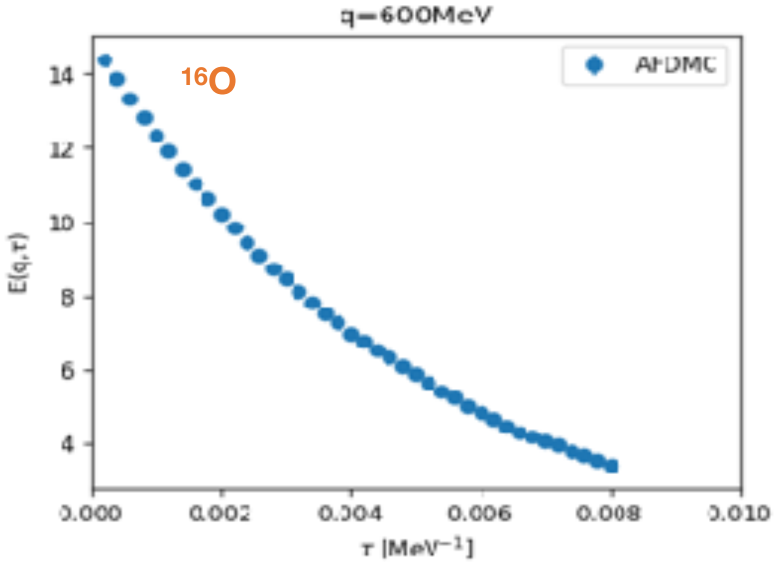

N. Rocco, AL et al., in preparation

BEYOND ^{12}C: AFDMC AND MACHINE LEARNING

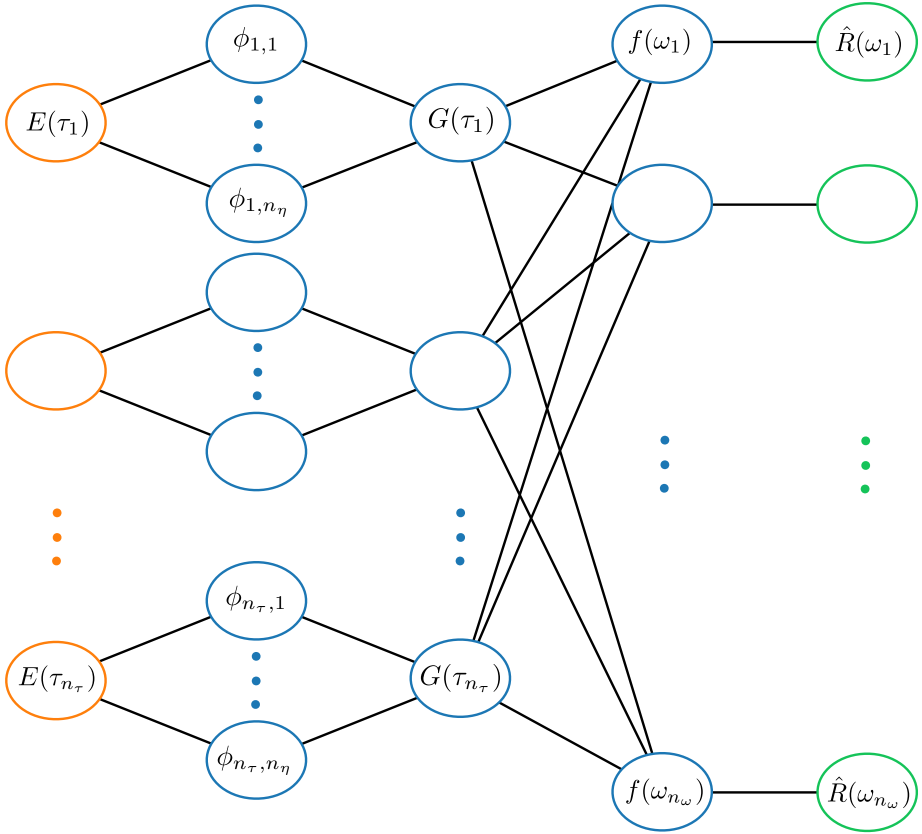

*K. Raghavan, AL, al., PRC **103**, 035502 (2021)*

Argonne NATIONAL LABORATORY

BEYOND ^{12}C: AFDMC AND MACHINE LEARNING

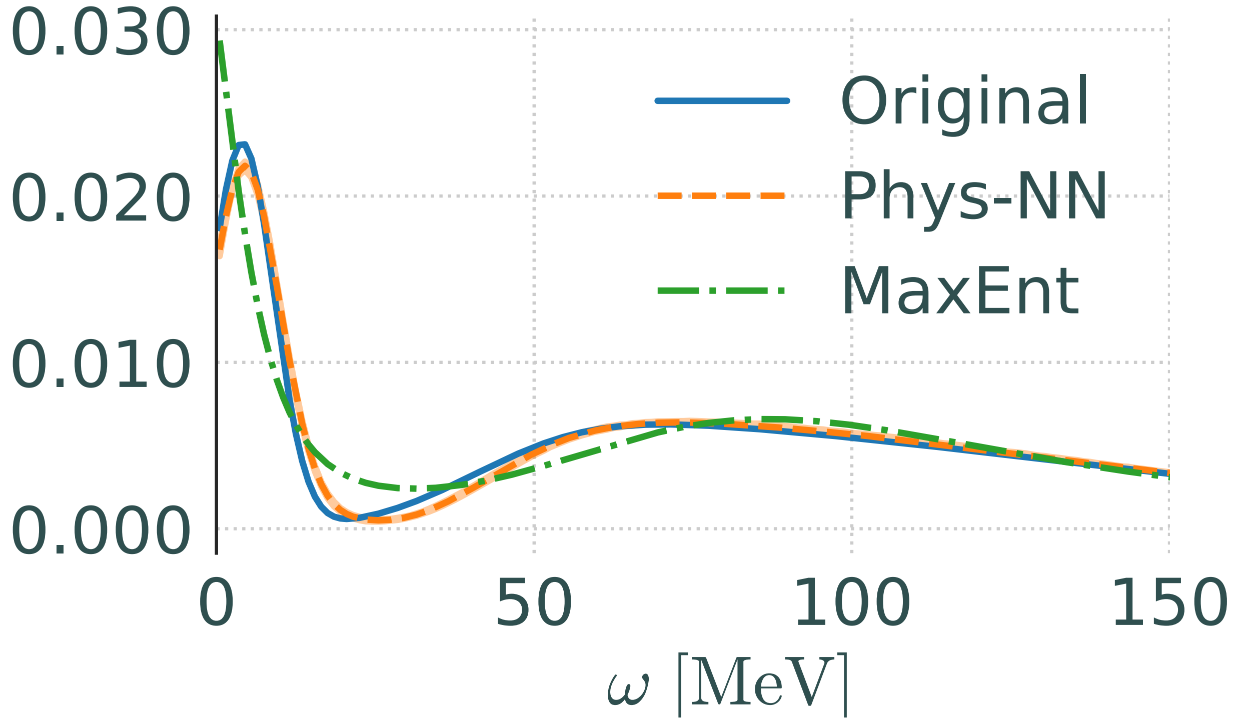

K. Raghavan, AL, al., PRC **103**, 035502 (2021)

BEYOND ^{12}C: AFDMC AND MACHINE LEARNING

We developed an artificial-neural network approach suitable to invert the Laplace transform that:

- Provides robust estimates of the uncertainty of the inversion;

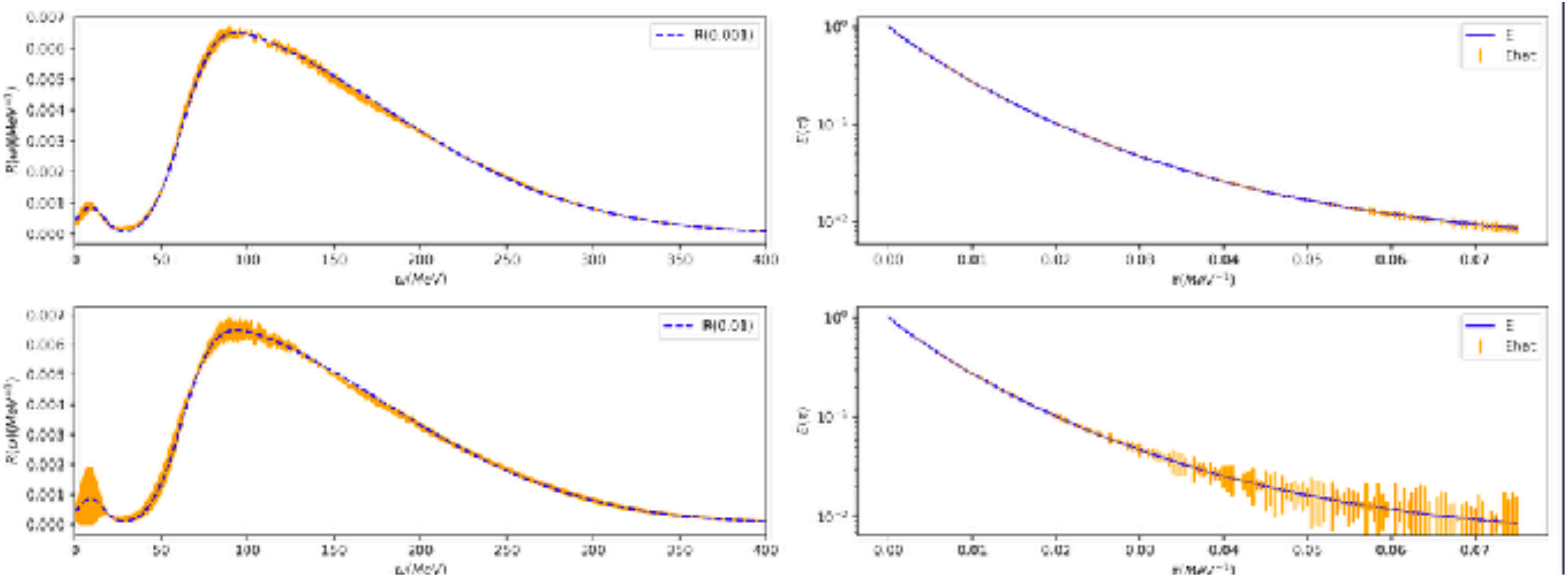

K. Raghavan, AL, in preparation)

HOW TO TACKLE (EVEN) LARGER NUCLEI?

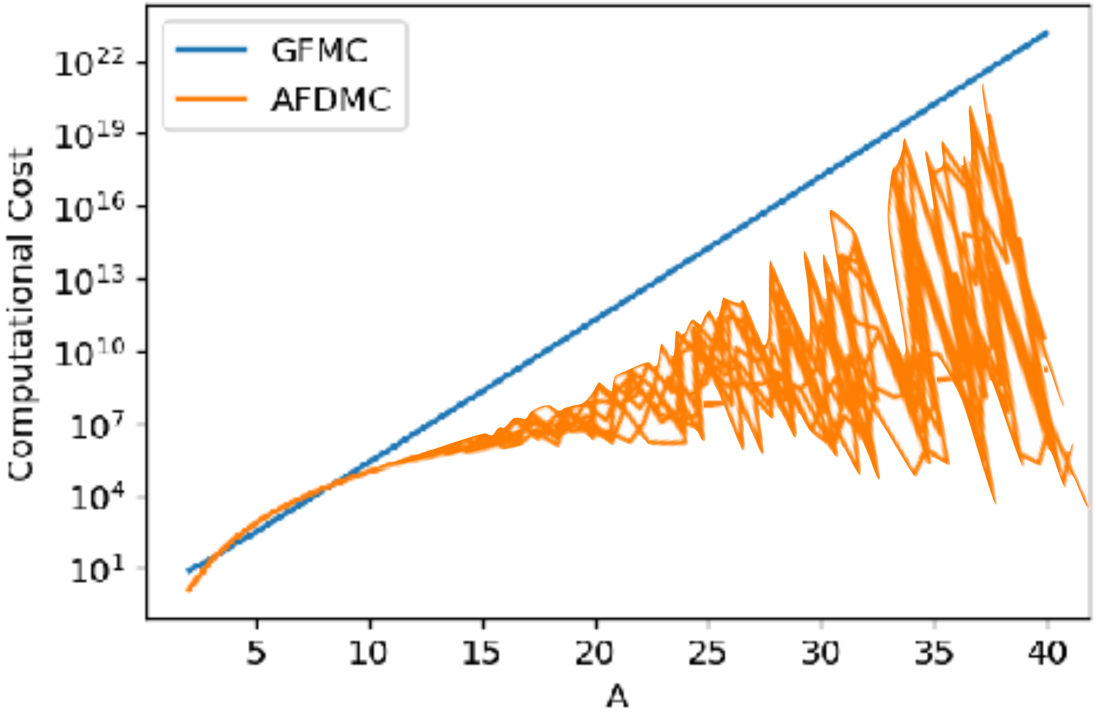

GFMC

$$|\Psi_T\rangle \sim \prod_{i<j} F_{ij}|\Phi\rangle$$

AFDMC

$$|\Psi_T\rangle \sim (1 + \sum_{i<j} F_{ij})|\Phi\rangle$$

NEURAL NETWORK QUANTUM STATES

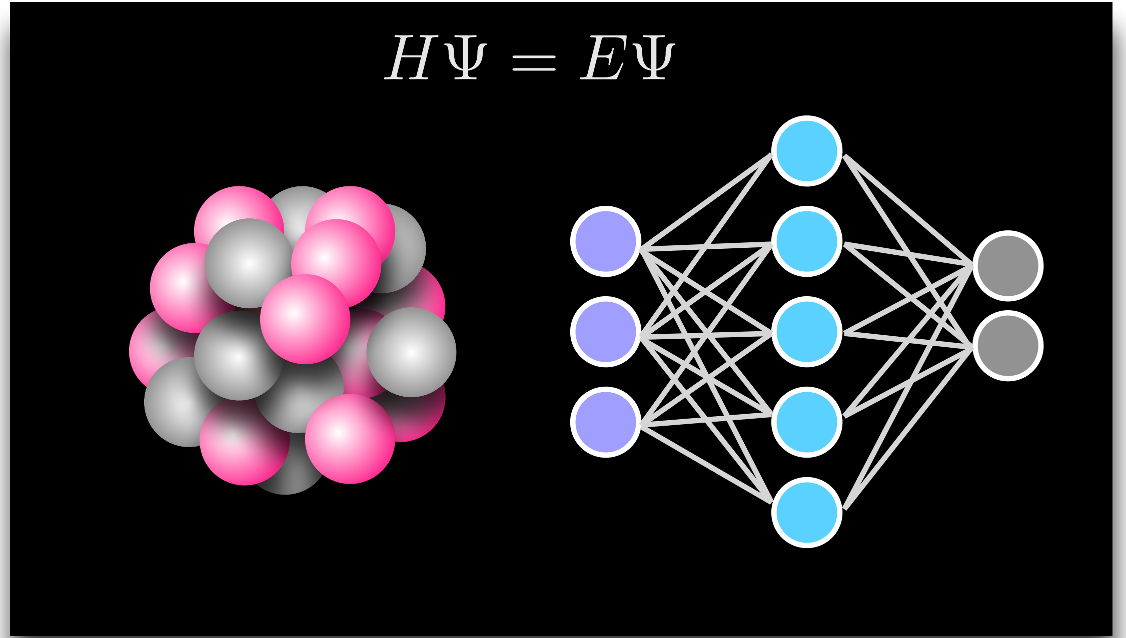

NEURAL-NETWORK QUANTUM STATES

The majority of quantum states of physical interest have distinctive features and intrinsic structures

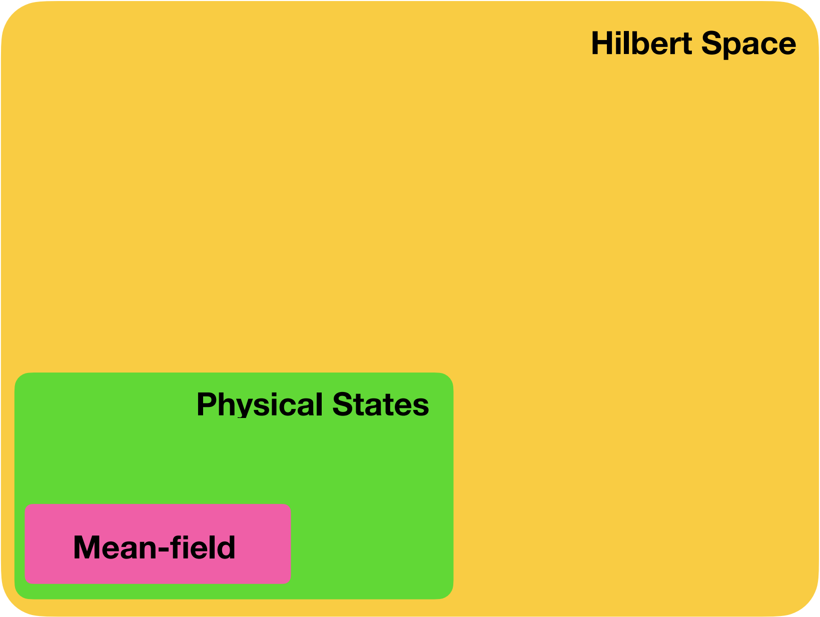

Artificial neural networks can compactly represent complex high-dimensional functions;

$$\Psi_0(X) \simeq \langle X|\hat{\Psi}(\mathbf{p})\rangle \equiv \hat{\Psi}(X,\mathbf{p})$$

- ANNs trained minimizing the energy

$$E(\mathbf{p}) = \frac{\langle\hat{\Psi}(\mathbf{p})|H|\hat{\Psi}(\mathbf{p})\rangle}{\langle\hat{\Psi}(\mathbf{p})|\hat{\Psi}(\mathbf{p})\rangle}$$

- MCMC used to sample the Hilbert space

$$E(\mathbf{p}) \simeq \sum_{X\sim|\Psi(X)|^2} \frac{\langle X|H|\hat{\Psi}(\mathbf{p})\rangle}{\langle X|\hat{\Psi}(\mathbf{p})\rangle}$$

NEURAL SLATER-JASTROW ANSATZ

The ANN variational state is a product of mean-field state modulated by a flexible correlator factor

$$\Psi_{SJ}(X) = e^{J(X)}\Phi(X)$$

- The mean-field part is a Slater determinants of single-particle orbitals

$$\det \begin{bmatrix} \phi_1(\mathbf{x}_1) & \phi_1(\mathbf{x}_2) & \cdots & \phi_1(\mathbf{x}_N) \\ \phi_2(\mathbf{x}_1) & \phi_2(\mathbf{x}_2) & \cdots & \phi_2(\mathbf{x}_N) \\ \vdots & \vdots & \ddots & \vdots \\ \phi_N(\mathbf{x}_1) & \phi_N(\mathbf{x}_2) & \cdots & \phi_N(\mathbf{x}_N) \end{bmatrix}$$

- Each orbital is a FFNN that takes as input

$$\bar{\mathbf{r}}_i = \mathbf{r}_i - \mathbf{R}_{CM}$$

- The Jastrow is a permutation-invariant function of the single-particle coordinates

$$J(X) = \rho_F\left[\sum_i \vec{\phi}_{\mathcal{F}}(\bar{\mathbf{r}}_i, \mathbf{s}_i)\right]$$

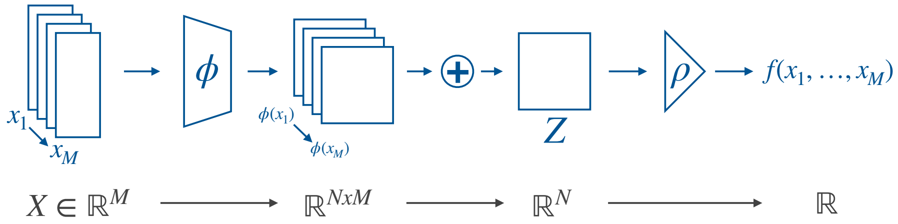

Wagstaff et al., arXiv:1901.09006 (2019)

Zaheer et al., arXiv:1703.06114 (2017)

STOCHASTIC RECONFIGURATION

The ANN is trained by performing an imaginary-time evolution in the variational manifold

$$(1 - H\delta\tau)|\Psi_V(\mathbf{p}_\tau)\rangle \simeq \Delta p^0 |\Psi_V(\mathbf{p}_\tau)\rangle + \sum_i \Delta p^i \frac{\partial}{\partial p^i} |\Psi_V(\mathbf{p}_\tau)\rangle$$

During the optimization, then parameter are updated as

$$\mathbf{p}_{\tau+\delta\tau} = \mathbf{p}_\tau - \eta(S_\tau + \epsilon I)^{-1}\mathbf{g}_\tau$$

The gradient is supplemented by the quantum Fisher Information pre-conditioner

$$\begin{cases} S_\tau^{ij} = \left\langle \dfrac{\partial \Psi_V(\mathbf{p}_\tau)}{\partial p_i} \middle| \dfrac{\partial \Psi_V(\mathbf{p}_\tau)}{\partial p_j} \right\rangle - \left\langle \dfrac{\partial \Psi_V(\mathbf{p}_\tau)}{\partial p_i} \right\rangle \left\langle \dfrac{\partial \Psi_V(\mathbf{p}_\tau)}{\partial p_j} \right\rangle \\ \gamma(\psi, \phi) = \arccos \sqrt{\dfrac{\langle\psi|\phi\rangle\langle\phi|\psi\rangle}{\langle\psi|\psi\rangle\langle\phi|\phi\rangle}} \end{cases}$$

S. Sorella, Phys. Rev. B ***64****, 024512 (2001)*

J. Stokes, at al., Quantum ***4****, 269 (2020).*

ADAPTIVE STOCHASTIC RECONFIGURATION

We use an adaptive learning rate with $10^{-7} < \eta < 10^{-2}$. It yields robust convergence patterns for all the nuclei and regulator choices that we have analyzed

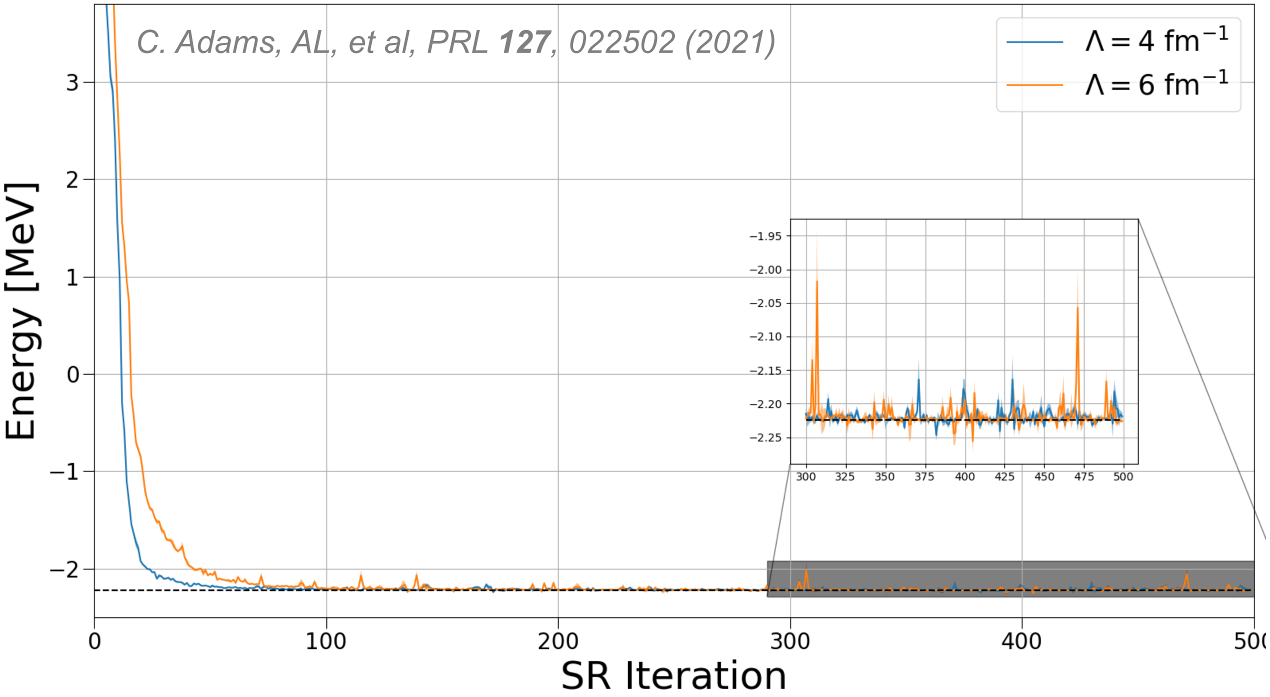

COMPARISON WITH QUANTUM MONTE CARLO

To further elucidate the quality of the ANN wave function we consider the point-nucleon density

$$\rho_N(r) = \frac{1}{4\pi r^2}\langle \Psi_V \Big| \sum_i \delta(r - |\mathbf{r}_i^{\mathrm{int}}|) \Big| \Psi_V \rangle \,,$$

^{3}H

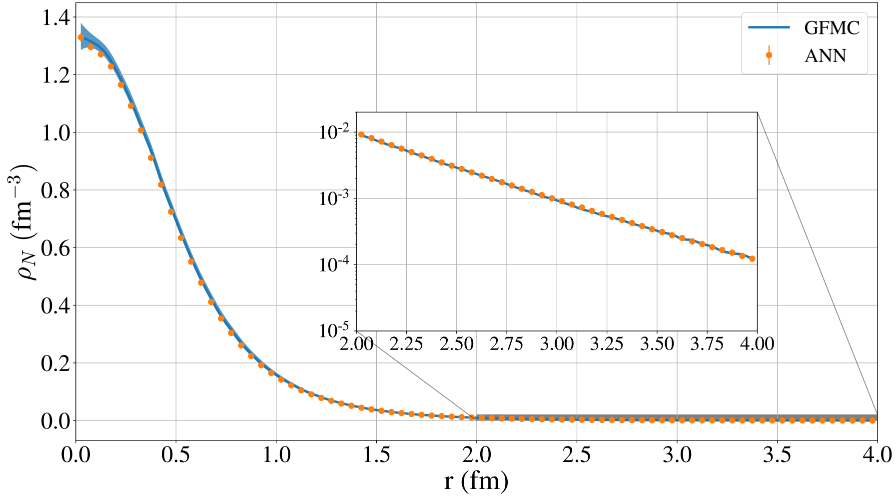

^{4}He

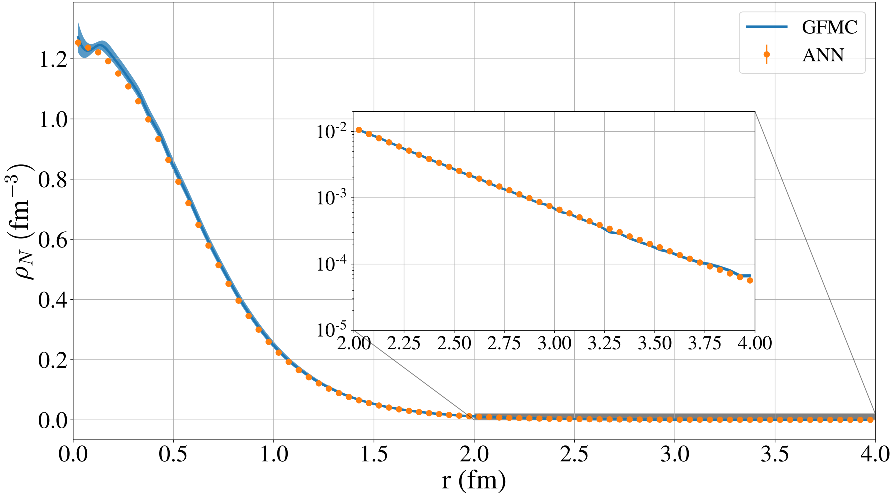

*C. Adams, AL, et al, PRL **127**, 022502 (2021)*

COMPARISON WITH QUANTUM MONTE CARLO

- The ANN Slater Jastrow ansatz outperforms conventional Jastrow correlations

	Λ	VMC-ANN	VMC-JS	GFMC	GFMC_c
^{2}H	4 fm^{-1}	$-2.224(1)$	$-2.223(1)$	$-2.224(1)$	-
	6 fm^{-1}	$-2.224(4)$	$-2.220(1)$	$-2.225(1)$	-
^{3}H	4 fm^{-1}	$-8.26(1)$	$-7.80(1)$	$-8.38(2)$	$-7.82(1)$
	6 fm^{-1}	$-8.27(1)$	$-7.74(1)$	$-8.38(2)$	$-7.81(1)$
^{4}He	4 fm^{-1}	$-23.30(2)$	$-22.54(1)$	$-23.62(3)$	$-22.77(2)$
	6 fm^{-1}	$-24.47(3)$	$-23.44(2)$	$-25.06(3)$	$-24.10(2)$

- Remaining differences with the GFMC are due to deficiencies in the Slater-Jastrow ansatz

$$\Psi_{SJ}(X) = e^{J(X)}\Phi(X)$$

C. Adams, AL, et al, PRL **127**, 022502 (2021)

HIDDEN NUCLEONS

The “hidden fermion” approach was recently introduced to model fermion wave functions

$$\langle RS|\Psi_{HF}\rangle = \begin{pmatrix} \phi_1(x_1) & \phi_1(x_2) & \phi_1(x_3) & \phi_1(x_4) & \phi_1(y_1) & \phi_1(y_2) & \phi_1(y_3) & \phi_1(y_4) \\ \phi_2(x_1) & \phi_2(x_2) & \phi_2(x_3) & \phi_2(x_4) & \phi_2(y_1) & \phi_2(y_2) & \phi_2(y_3) & \phi_2(y_4) \\ \phi_3(x_1) & \phi_3(x_2) & \phi_3(x_3) & \phi_3(x_4) & \phi_3(y_1) & \phi_3(y_2) & \phi_3(y_3) & \phi_3(y_4) \\ \phi_4(x_1) & \phi_4(x_2) & \phi_4(x_3) & \phi_4(x_4) & \phi_4(y_1) & \phi_4(y_2) & \phi_4(y_3) & \phi_4(y_4) \\ \chi_1(x_1) & \chi_1(x_2) & \chi_1(x_3) & \chi_1(x_4) & \chi_1(y_1) & \chi_1(y_2) & \chi_1(y_3) & \chi_1(y_4) \\ \chi_2(x_1) & \chi_2(x_2) & \chi_2(x_3) & \chi_2(x_4) & \chi_2(y_1) & \chi_2(y_2) & \chi_2(y_3) & \chi_2(y_4) \\ \chi_3(x_1) & \chi_3(x_2) & \chi_3(x_3) & \chi_3(x_4) & \chi_3(y_1) & \chi_3(y_2) & \chi_3(y_3) & \chi_3(y_4) \\ \chi_4(x_1) & \chi_4(x_2) & \chi_4(x_3) & \chi_4(x_4) & \chi_4(y_1) & \chi_4(y_2) & \chi_4(y_3) & \chi_4(y_4) \end{pmatrix}$$

Visible orbitals on visible coordinates

Visible orbitals on hidden coordinates

Hidden orbitals on visible coordinates

Hidden orbitals on hidden coordinates

*J. R. Moreno, et al., PNAS **119,** 2122059119(2022)*

HIDDEN NUCLEONS

The “hidden fermion” approach was recently introduced to model fermion wave functions

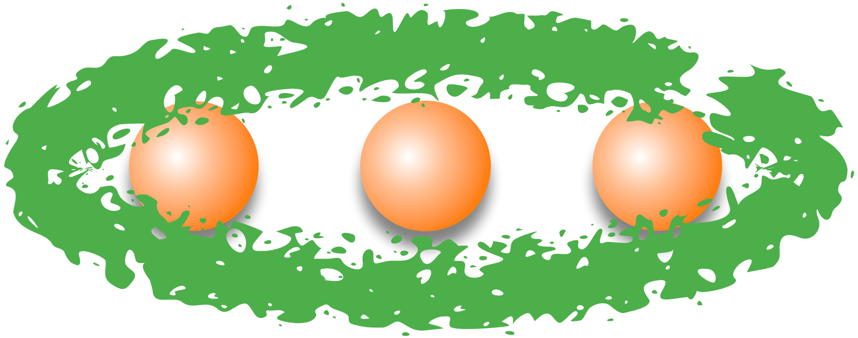

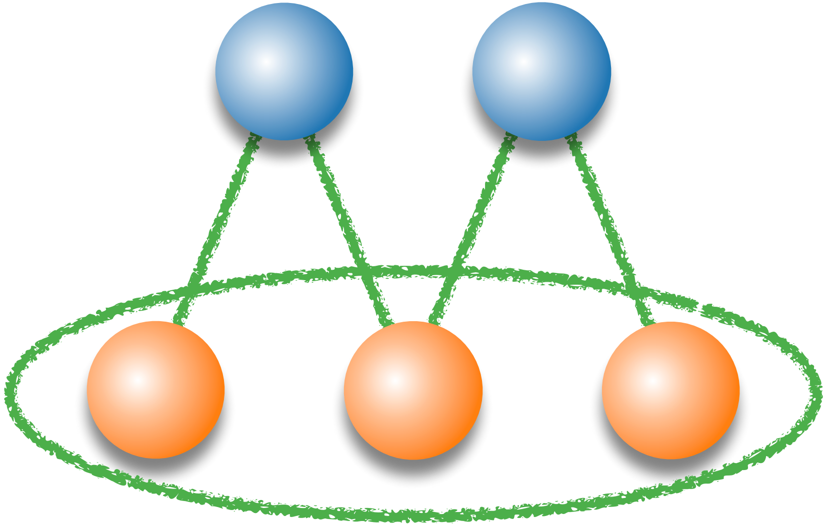

HIDDEN NUCLEONS

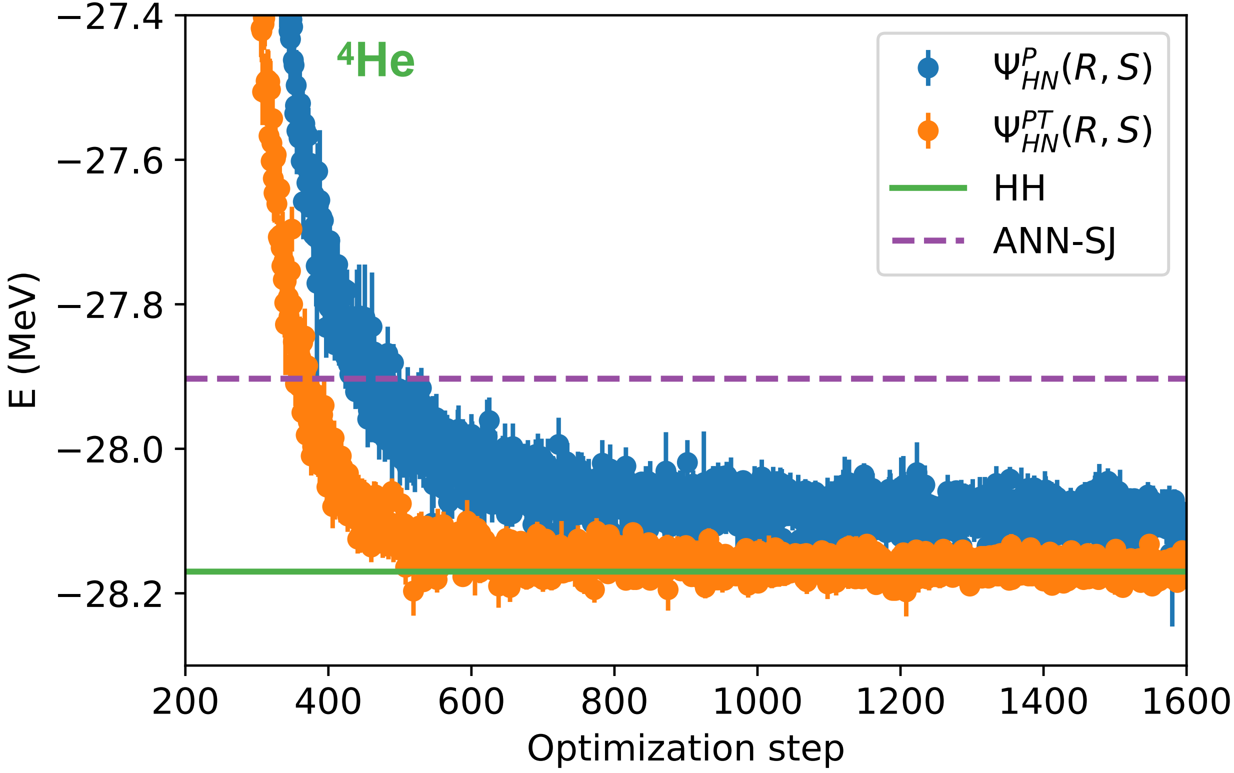

AL, et al., Phys.Rev.Res. ***4*** *(2022) 4, 043178*

HIDDEN NUCLEONS

We extend the reach of neural quantum states to ^{16}O

In addition to its ground-state energy, we evaluate the point-nucleon density of ^{16}O with A_h=16

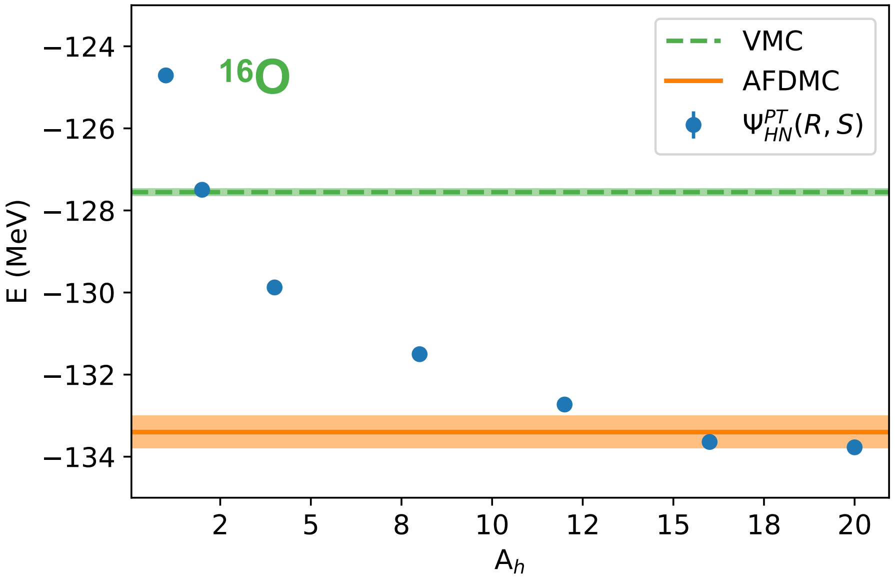

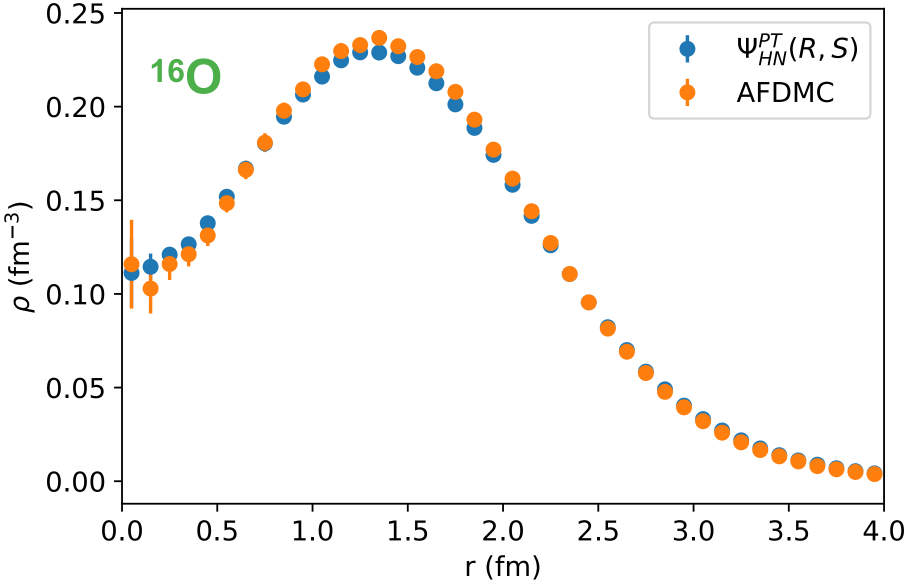

AL, et al., Phys.Rev.Res. ***4*** *(2022) 4, 043178*

DILUTE NEUTRON MATTER

We have introduced a periodic hidden-nucleons ansatz to model low-density neutron matter

The NQS ansatz converges to the unconstrained AFDMC energy, using a fraction of the computing time

- NQS: 100 hours on NVIDIA-A100
- AFDMC: 1.2 million hours on Intel-KNL

The hidden-nucleon ansatz captures the overwhelming majority of the correlation energy

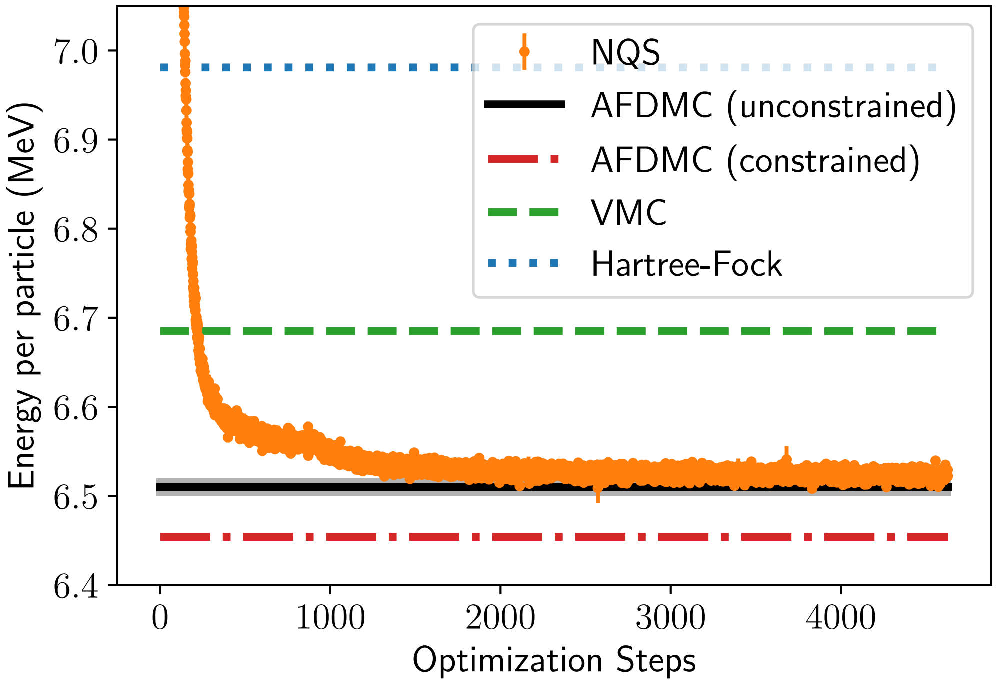

B. Fore, J. Kim, AL, arXiv:2212.04436 [nucl-th]

MESSAGE-PASSING NEURAL NETWORK

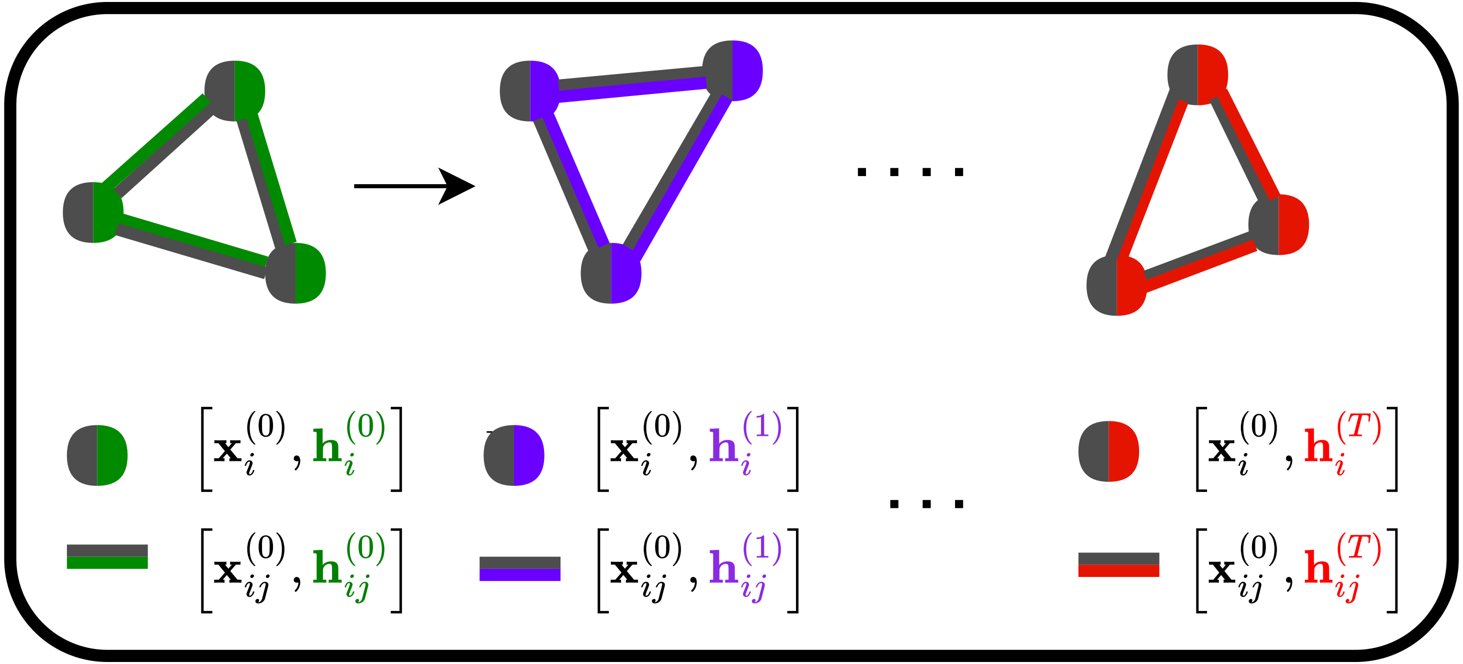

G. Pescia, et al., 2305.08831 [cond-mat.quant-gas]

NUCLEI WITH MPNN

In addition to energies and single-particle densities, we can compute electroweak properties

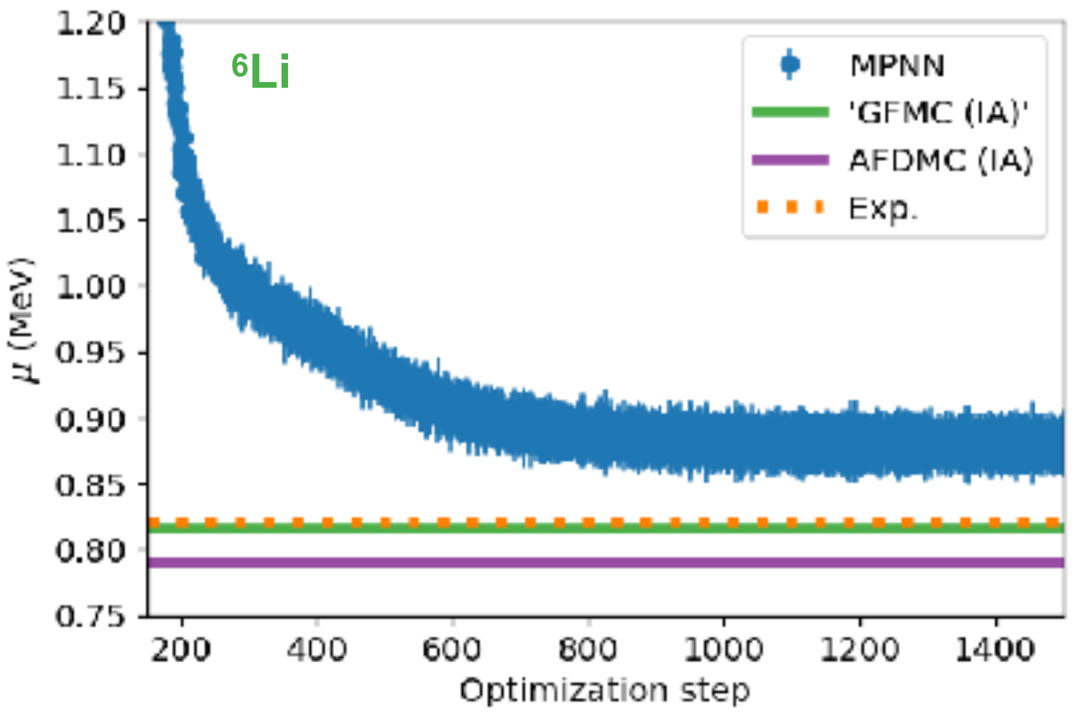

A. Gnech, AL, in preparation

NUCLEI WITH MPNN

In addition to energies and single-particle densities, we can compute electroweak properties

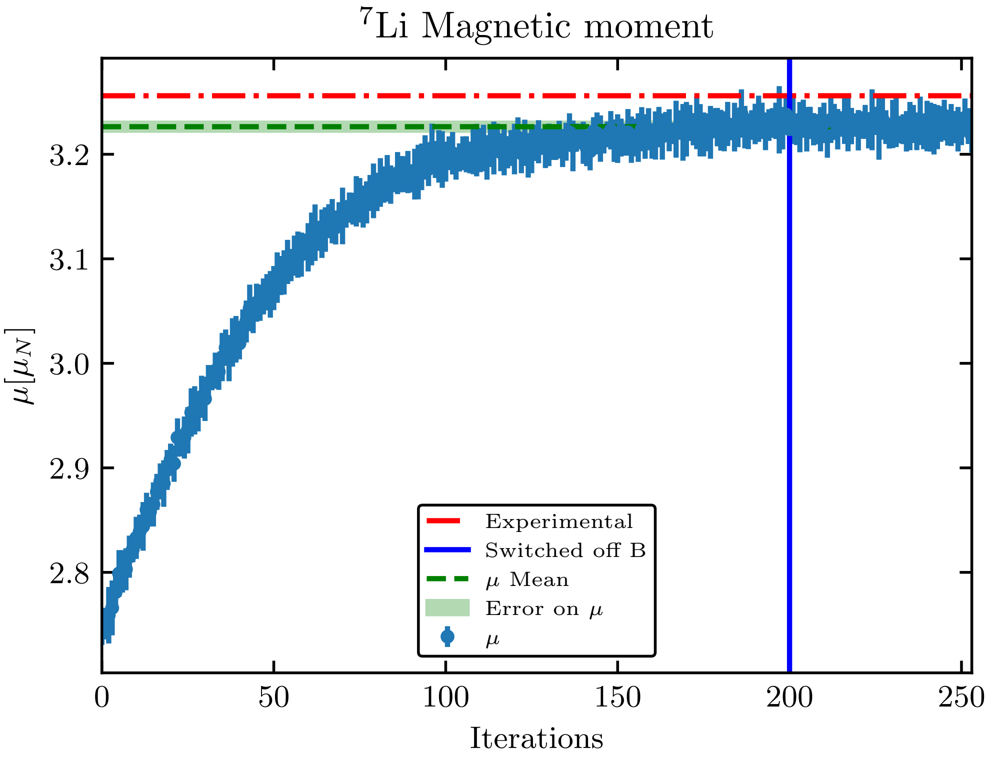

NUCLEI WITH MPNN

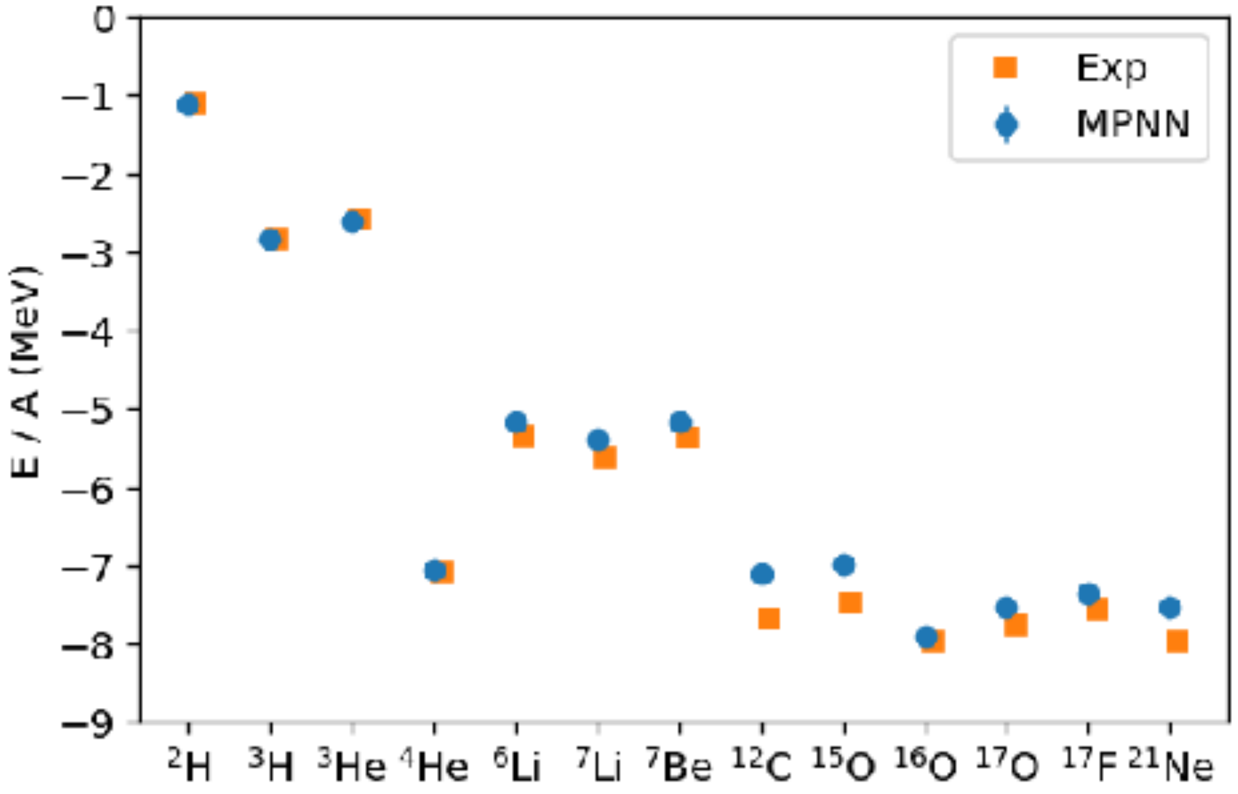

NUCLEI WITH MPNN

Even with just one hidden-nucleon we do better than AFDMC for medium-mass nuclei

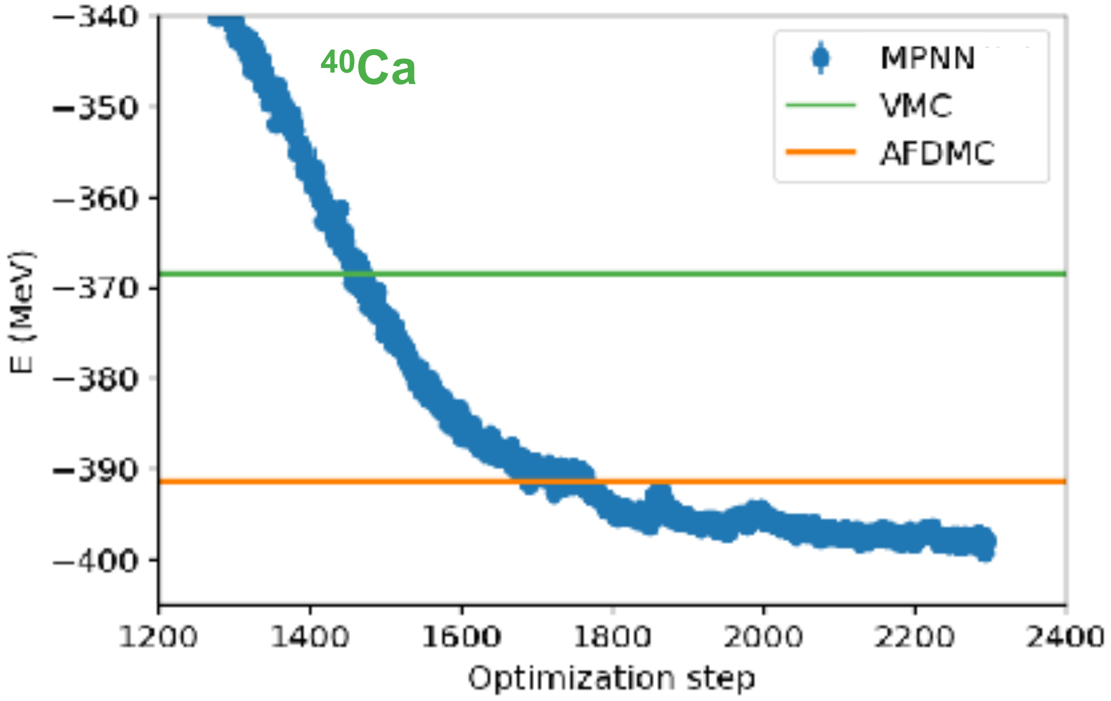

CONCLUSIONS

Neural network quantum states are extending the reach of conventional QMC methods

- Favorable scaling with the number of fermions;
- Universal and accurate approximations for fermion wave functions;
- Suitable for confined and periodic systems;
- Scalable to leadership-class hybrid CPU/GPU computers

PERSPECTIVES

- Access "real-time" dynamics: the prototypal exponentially-hard problem in many-body theory

$$\mathcal{D}\left(|\Psi(\mathbf{p}_{t+\delta t})\rangle, e^{-iHt}|\Psi(\mathbf{p}_t)\rangle\right)^2 = \arccos\left(\sqrt{\frac{\langle\Psi(\mathbf{p}_{t+\delta t})|e^{-iHt}|\Psi(\mathbf{p}_t)\rangle\langle\Psi(\mathbf{p}_t)|e^{iHt}|\Psi(\mathbf{p}_{t+\delta t})\rangle}{\langle\Psi(\mathbf{p}_{t+\delta t})|\Psi(\mathbf{p}_{t+\delta t})\rangle\langle\Psi(\mathbf{p}_t)|\Psi(\mathbf{p}_{\tau+\delta t})\rangle}}\right)^2$$

- Relevant for: lepton-nucleus scattering, fusion, and collective neutrino oscillation;

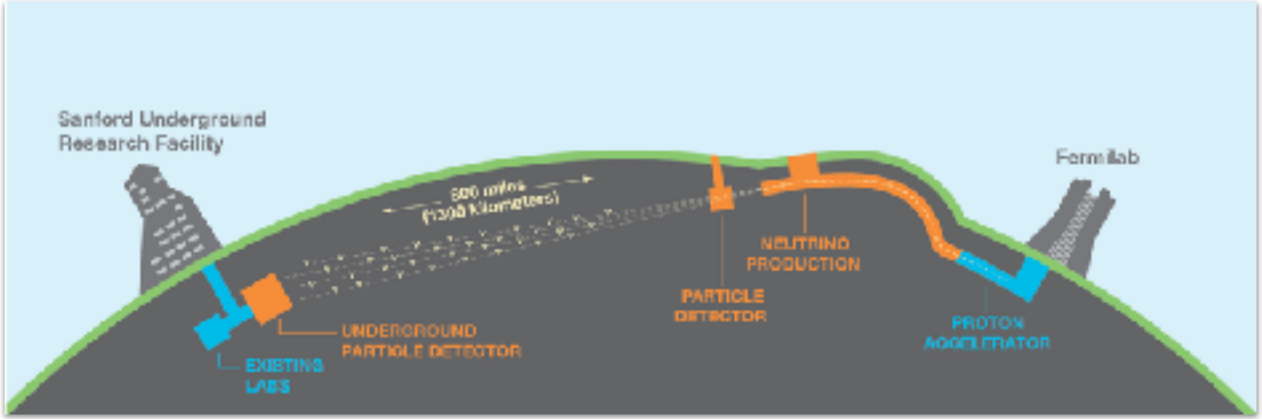

THANK YOU